Department of Molecular Medicine
PhD program in Human Biology and Medical Genetics-XXXVII cycle

The RNA binding protein PCBP2 is a regulator of miRNAs partition between cell and extracellular vesicles

Candidate:
Dr. Francesco Marocco

Scientific tutor:
Prof. Cecilia Battistelli

Director of PhD program
Prof. Laura Stronati

Academic year 2023-2024

SUMMARY

ABSTRACT

In recent years, growing interest has focused on Extracellular Vesicles (EVs) as regulators of cell-to-cell communication: EVs are able to promote changes in gene expression and behavior of recipient cells in several pathophysiological processes by transferring their specific informational cargo of molecules. EVs cargo does not simply reflect the cell of origin content, but rather is defined by dynamic and selective cell-specific loading mechanisms. In particular, it is well recognized that EVs-mediated transfer of microRNAs contributes to intercellular communication, however, the knowledge about molecular mechanisms regulating selective and dynamic miRNA-loading in EVs is limited to a few specific RNA-binding proteins (RBPs) interacting with specific sequence determinants. Moreover, although several sequence motifs causing intracellular retention have been disclosed, the identification of interacting proteins remains unaddressed. Starting from this body of evidence, we focused on the investigation of molecular players responsible for miRNAs intracellular retention.

Here, the RBP Poly-C-binding protein 2 (PCBP2, also known as hnRNPE2 or αCP2) was identified as a direct interactor of an intracellular retention (CELL) motif: RNA immunoprecipitation (RIP)

after UV cross-linking, coupled to RNA pull-down followed by proteomic analysis, demonstrated that this protein directly binds to miRNAs embedding this sequence and mutagenesis of the motif proved the specificity of its binding. Functionally, PCBP2 knock-down allows the EV-loading of specific intracellular microRNAs.

Furthermore, a second requirement for PCBP2 specific binding was identified in SYNCRIP, a previously characterized miRNA EV-loader. SYNCRIP and PCBP2 may contemporarily bind to miRNAs endowed of both hEXO and CELL motifs, as demonstrated by RIP and EMSA assays. Mechanistically, SYNCRIP knock-down appears to limit PCBP2 recruitment.

Overall, this body of evidence highlights that multiple proteins/miRNA interactions govern miRNA compartmentalization and, specifically, extends PCBP2's known pleiotropic functions to that of intracellular determinant of miRNAs retention, as a dominant inhibitor of SYNCRIP function.

INTRODUCTION

EXTRACELLULAR VESICLES

Extracellular vesicles (EVs) are a heterogeneous group of membrane-bound particles released by cells into the extracellular space, evolutionarily conserved from bacteria to humans and plants[1-3], differing in size, cargo, surface characteristics and intracellular origin[4]. Based on their biogenesis, EVs are classified into two main populations: microvesicles and exosomes[5].

Microvesicles (MVs), formerly called 'platelet dust', have a role in cell–cell communication in various cell types, including cancer cells, where they are generally called oncosomes. Microvesicles range in size from 50 nm to 1000 nm in diameter but can be even larger (up to 10 μm) in the case of oncosomes. They are generated by the outward budding and fission of the plasma membrane and the subsequent release of vesicles into the extracellular space[6].

Exosomes, characterized by a range in size from 30 nm to 150 nm of diameter, are, instead, intraluminal vesicles (ILVs) formed by the inward budding of the endosomal membrane during maturation of multivesicular endosomes (MVEs), which are intermediates within

the endosomal system, and secreted upon fusion of MVEs with the cell surface[7].

Apoptotic bodies that form when cells fragment during programmed cell death are also categorized as EVs; they are the largest of EV groups, with a typical size spanning between 1000 and 5000 nm. These vesicles contain DNA fragments, histones, chromatin remnants, cytosolic fractions, and degraded proteins. Typically, apoptotic bodies are cleared by phagocytic cells[8] (figure 1).

Because these EV subtypes can be difficult to distinguish from each other on the basis of biochemical preparations, the latest classification guidelines recommend describing purified EVs as "small" and "large" EVs[9].

Despite a different pathway of biogenesis, exosomes and microvesicles display a similar appearance, overlapping size and often common composition that make it difficult to ascertain their origin once isolated from the extracellular medium or from biological fluids. EVs are highly abundant in cytoskeletal, cytosolic, heat shock and plasma membrane proteins, as well as in proteins involved in vesicle trafficking (e.g. tetraspanins, 14.3.3 proteins, Tsg101 and Alix), while intracellular organelle proteins are less abundant[10].

These proteins, present in the majority of EVs, reflect vesicle localization, cellular origin and mechanisms of secretion. For these reasons, some of them, although not specifically present in

microvesicles or exosomes, are used as markers to distinguish the different EVs subpopulations on the basis of their abundance and/or the specific contemporary expression. For example, the combination of the tetraspanins CD9, CD63 and CD81 is used as a marker for exosomes, while the combination of CD9, CD63 and CD82 identifies microvesicles. Moreover, while Tsg101 and Alix are more abundant in exosomes as they are components of the endosomal trafficking, Calnexin is considered a marker for microvesicles as it is a component of the ER, through which the proteins incorporated into microvesicles pass[11].

In addition to the proteins already mentioned above, EVs contain MHC class I and II molecules, membrane transport and fusion proteins (e.g., GTPases, annexins, flotillin, Rab2, Rab7, Rab11).

Lipid rafts, such as glycosylphosphatidylinositol anchored proteins (LBPA) and flotillin, are highly enriched in exosomes. Moreover, metabolic enzymes, such as GAPDH, enolase 1, PKM2, and PGK1, and molecules involved in signal transduction, such as protein kinases, 14-3-3, and G proteins, have been detected[11,12].

With respect to the EVs' molecular cargo, it is characterized by proteins, RNA, lipids and DNA and varies depending on the cell of origin, tissue types and pathophysiological conditions.

Indeed, apart from proteins, EVs also contain RNAs, including messenger RNAs (mRNAs), microRNAs (miRNAs)[13], long non-

coding RNAs (lncRNAs)[14], as well as mitochondrial DNA[15], small fragments of single-stranded DNA and large fragments of genomic, double-stranded DNA encompassing all chromosomes[16,17].

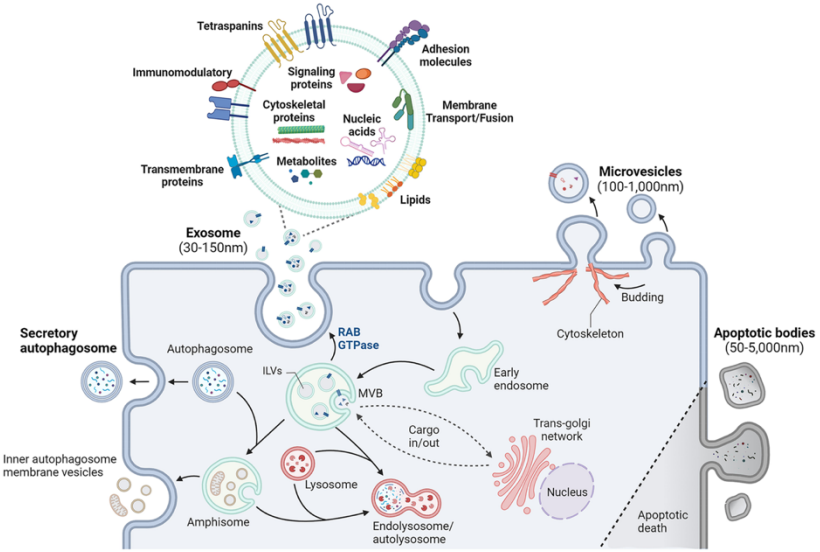

Figure 1. Main features of extracellular vesicles
EVs comprise a heterogeneous population of membrane vesicles of various origins characterized by different size, morphology and cargo content
(From Lee, Y.J. et al. Exp Mol Med 2024)

1.1 Exosomes biogenesis

Exosomes are generated as ILVs within the lumen of endosomes during their maturation into MVEs, a process that involves specific

sorting machineries. These machineries first segregate cargoes on microdomains of the MVEs limiting membrane, with consequent inward budding and fission of small membrane vesicles containing sequestered cytosol (figure 2).

The protein sorting of ILVs is a highly regulated process depending on the endosomal sorting complex required for transport (ESCRT) machinery[18]. The ESCRT pathway involves the coordinated action of all four ESCRT complexes (ESCRT-0, ESCRT-I, ESCRT-II, and ESCRT-III), which act in a stepwise manner, in conjunction with disassembly and deubiquitylating enzymes present on the endosome membrane. This process also involves the ESCRT accessory protein VPS4[19]. ESCRT-0, -I, and -II complexes are equipped with ubiquitin-binding domains that allow them to capture ubiquitinated cargo[20]. Moreover, ESCRT-I, -II, and -III play crucial roles in membrane remodeling for ILVs binding. To complete exosome biogenesis, ESCRT-II induces the formation of ESCRT-III filaments, which facilitate the severing of the nascent exosome neck from the endosome membrane[21]. ESCRT-III is thought to be directed to the vesicle bud neck, either by sensing negative membrane curvature or by promoting membrane bending, to facilitate the separation of ILVs from the endosome membrane[22].

The ATPase VPS4 interacts with ESCRT-III to facilitate the final stages of ILVs formation by promoting membrane scission, resulting in the leakage of ILVs into the multivesicular bodies (MVB) lumens.

Importantly, the deletion of multiple ESCRT protein subunits or VPS4 can significantly impact exosome biogenesis, leading to alterations in exosome number, size, and protein composition to varying extents. The roles of ESCRT proteins in ILVs biogenesis are conserved, as evidenced by studies in budding yeast, where deletion of ESCRT proteins results in pre-vacuolar, endosomal compartments that lack ILVs[23].

Exosomes can also be formed in an ESCRT-independent manner: the first ESCRT-independent mechanism of exosome biogenesis was shown to require generation of ceramide by neutral type II sphingomyelinase (nSMase2), which hydrolyses sphingomyelin to ceramide[24]. Ceramide may then allow the generation of membrane subdomains, which impose a spontaneous negative curvature on the membranes[25]. Recently, activated Rab31 GTPase was identified as the trigger for membrane budding within these domains[26].

A second class of molecules, the tetraspanins, participates in various steps of the exosome biogenesis pathway, such as in directing cargo toward multi vesicular bodies (MVBs), compartmentalizing endosomal membrane into functional domains named tetraspanin-enriched microdomains (TEMs), and increasing exosome secretion of certain compounds, such as beta-catenin[27,28]. Recent structural analysis of the tetraspanin CD81 revealed a cone-like structure with an intramembrane cavity that can accommodate cholesterol and that

is likely to be shared by other tetraspanins. Clustering of several cone-shaped tetraspanins in combination with different transmembrane and cytosolic proteins could induce inward budding of the microdomain in which they are enriched[29].

Additional ESCRT-independent mechanisms contribute to the targeting of selective soluble or membrane-associated cargoes to exosomes. For example, the sequestration of cytosolic proteins into ILVs can result from co-sorting with other proteins, such as the chaperones heat shock 70 kDa protein (HSP70) and heat shock cognate 71 kDa protein (HSC70), which are found in exosomes derived from most cell types[30].

Moreover, recent insights have shed light on variation in ESCRT pathway as the syndecan-syntenin-ALIX pathway: in MCF7 breast cancer cells, syntenin, a cytoplasmic adapter protein, recruits ALIX to MVBs, where its interaction with ESCRT-III induces ILVs formation. Regulation of syndecan-syntenin-ALIX-mediated exosome biogenesis involves activation of the oncogenic tyrosine kinase SRC that phosphorylates syndecan1, syntenin, and ALIX, thereby stimulating exosome biogenesis[31,32].

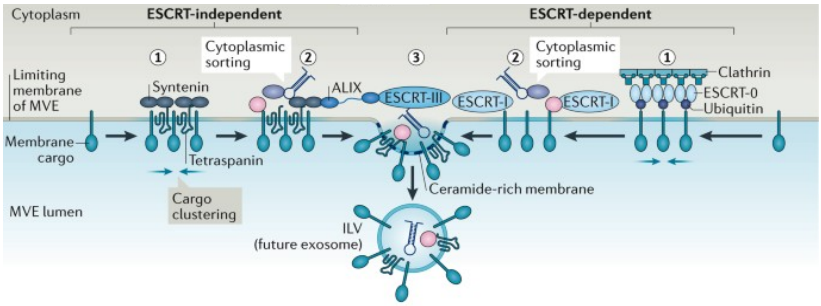

Figure 2. Biogenesis of exosomes
Several sorting machineries involved in the different steps required for generating exosomes
(Modified from Van Niel G. et al., Nat. Rev. Mol. Cell Biol., 2018)

1.2 The release of exosomes

MVEs are primarily destined to fuse with lysosomes as a protein degradation mechanism (in addition to the ubiquitin-proteasome system)[33]; however, mechanisms preventing their degradation and allowing MVEs' secretion exist, thereby enabling exosomes' release (figure 3). The regulation of the balance between degradative and secretory capacity of MVEs remains largely unexplored, but the establishment of this balance undoubtedly affects cell function. For example, lysosomal degradation defects that promote exosome secretion have been shown to enable efficient elimination of unwanted and/or defective proteins such as amyloids in the context of

neurodegenerative diseases[34]. A first level of regulation of the balance is probably mediated by the sorting machineries at the level of MVEs. In fact, while the different components of the ESCRT machinery are generally associated with the degradative pathway of MVEs, the syndecan-syntenin-Alix pathway seems to be restricted only to exosome secretion. Conversely, ISGylation (a ubiquitin-like modification) of the ESCRT-I component TSG101 induces its aggregation and degradation, being sufficient to impair exosome secretion[35].

MVEs fated to exosomes secretion need to move toward the plasma membrane: there are a few key players in this vesicular traffic system: actin filaments and microtubules, along which the vesicles move, motor proteins, such as kinesin and dynein, which directly facilitate the movement, and Rab family of small GTPases which recruit and activate the motor proteins[36]. The main RAB GTPases that have been shown to be involved in the production and secretion of exosomes are RAB27A and B. Specifically, RAB27B regulates the motility of MVEs towards the plasma membrane, while both RAB27 isoforms are involved in the step following MVE transport, represented by the docking at the plasma membrane to promote the fusion propaedeutic to the exosome secretion. The role of RAB27A in MVE docking involves rearrangement of sub-membrane actin cytoskeleton, a step that is common to all mechanisms involving vesicular secretion[37].

Exosome secretion requires the fusion of MVEs with the plasma membrane to release ILVs as exosomes, a process probably mediated by SNARE proteins and synaptotagmin family members[38]. In MCF-7 breast cancer cells, syntaxin-4, SNAP-23, and VAMP-7 are the SNAREs responsible for exosome secretion and SNARE complex consisting of these SNAREs can drive membrane fusion *in vitro*. Deletion of any of these SNAREs in MCF-7 cells did not affect MVBs' biogenesis and transportation, indicating their specific involvement in the following steps driving the MVBs–plasma membrane fusion. In addition, syntaxin-4, SNAP-23, and VAMP-7 play equivalent roles in exosome secretion in both HeLa cervical cancer cells and A375 melanoma cells, suggesting their conserved function in exosome secretion[39]. Additional SNARE proteins involved in exosome secretion, such as the synaptobrevin homologue Ykt6[40], in Drosophila, syntaxin 5 in C. elegans[41] and syntaxin 1a[42] in mammals, again reflect the diversity of regulators that could be involved in exosome secretion, most likely depending on the organism, the cell type or the MVEs' subtype.

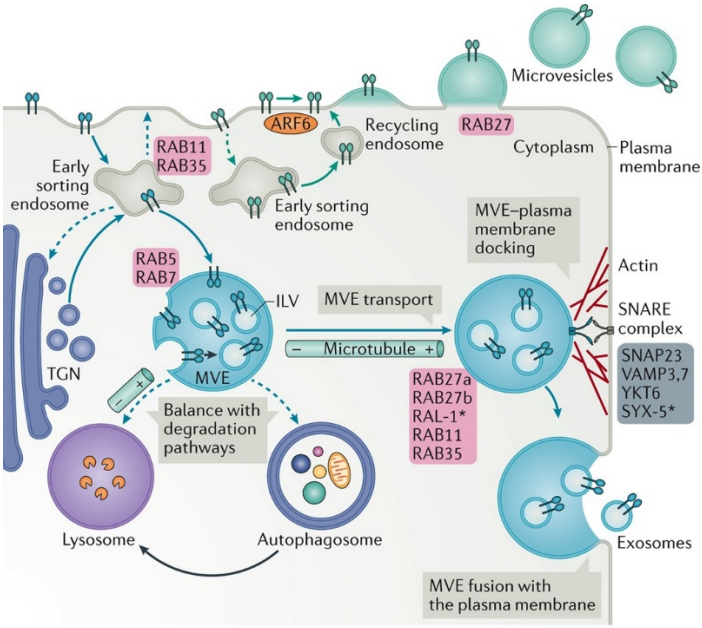

Figure 3. Intracellular trafficking of extracellular vesicles
The generation of EVs requires tuned regulation of multiple intracellular trafficking steps that influence the targeting of cargoes to the site of extracellular vesicle biogenesis and the fate of the multivesicular endosome (MVE) from which these vesicles originate.
(From Van Niel G. et al., Nat. Rev. Mol. Cell Biol., 2018)

1.3 Fate of extracellular vesicles in recipient cells

Once released into the extracellular space, extracellular vesicles can reach recipient cells and deliver their contents to elicit functional responses and promote phenotypic changes that will affect their

physiological or pathological status. Extracellular-vesicle-mediated intercellular communication requires docking at the plasma membrane, followed by the activation of surface receptors and consequent signaling, vesicle internalization (endocytosis) or their fusion with target cells[11] (figure 4).

The transmembrane ligands on exosome surface can directly bind to the surface receptors on the recipient cell and generate downstream signaling cascade to activate the target cell. This is a common route to mediate immunomodulatory and apoptotic functions. Exosomes released from dendritic cells activate T lymphocytes through MHC-peptide complex and bind to Toll-like receptor ligands on bacterial surface to activate bystander dendritic cells and to enhance immune responses[43,44].

Exosomes can also fuse with the plasma membrane and release their content directly into the cytosol of target cells. This includes hemi-fusion stalk formation between hydrophobic lipid bilayers of the exosome and plasma membrane followed by an expansion forming one consistent structure. Families of SNAREs and Rab proteins likely mediate this fusion, as shown in several studies on cell membrane[45].

Uptake via endocytosis can be categorized into different types of endocytotic processes, including clathrin-mediated endocytosis, caveolin-mediated endocytosis, lipid raft-mediated endocytosis, macropinocytosis, and phagocytosis. The uptake of EVs may be

dependent on the cell type and its physiologic state, and on the presence of ligands on the surface of the EVs, recognizing receptors on the surface of the cell or vice versa[46].

Clathrin-mediated endocytosis is a stepwise assembly of various transmembrane receptors and ligands. This process is characterized by the involvement of the triskelion scaffold (clathrin), leading to the formation of clathrin-coated vesicles[7]; the internalized vesicles undergo uncoating and fuse with endosomes[47]. This mode of EVs entry occurs in most cell types.

Caveolin-mediated endocytosis is mediated by integral membrane proteins named caveolins, which create small flask- or omega-shaped plasma membrane invaginations called caveolae. Caveolae enable internalization of caveosomes, which are large vesicles enriched in highly hydrophobic and detergent-resistant membrane lipids containing cholesterol and sphingolipids[48,49].

Lipid raft-mediated endocytosis is a major endocytic mechanism to shift cargo into early endosomes and influence EVs uptake. Lipid rafts are detergent-resistant membrane microdomains enriched in cholesterol, sphingolipids, and glycosylphosphatidylinositol-anchored proteins. They act not only as organizing centers for the assembly of signaling molecules, but also affecting membrane fluidity and mediating membrane protein trafficking[50].

Phagocytosis typically engulfs large particles, such as bacteria and dead cells, but can also internalize small particles like EVs[51]. Phagocytosis is an actin-mediated mechanism and a receptor-mediated event that is often performed by specialized cells such as macrophages. Phagocytosis is a stepwise process whereby cell membrane deformations encircle the bulk extracellular particles, forming phagosomes that eventually direct internalized cargo to lysosomes[46]. Meanwhile, macropinocytosis uses actin-driven lamellipodia to induce inward plasma membrane invaginations that get pinched off to form intracellular compartments called macropinosomes. They are growth factor-dependent and result in the nonspecific uptake of extracellular soluble molecules, nutrients, and antigens[52].

Upon internalization, exosomes follow the endocytic pathway and reach MVEs, which, in most cases, are targeted to the lysosomes. In this way, degradation of proteins and lipids carried by exosomes can provide a relevant source of metabolites to the recipient cell. However, in some cases, the internalized vesicles may escape digestion by back fusion with the limiting membrane of the MVEs, thereby releasing their contents into the cytoplasm of the recipient cell[7,53].

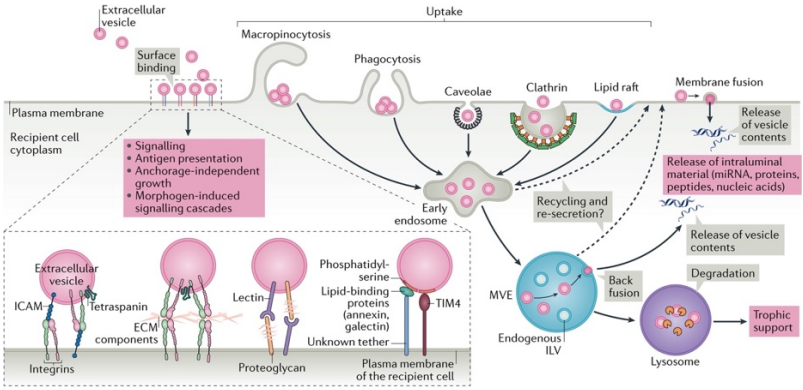

Figure 4. Fate of extracellular vesicles in recipient cells
In the recipient cell exogenous extracellular vesicles will bind to the cell surface and can undergo various fates.
(From Van Niel G. et al., Nat. Rev. Mol. Cell Biol., 2018)

1.4 Extracellular vesicles in pathophysiological conditions

Extracellular vesicles (EVs) are increasingly being recognized as mediators of intercellular communication by transferring their specific informational cargo of molecules, promoting changes in gene expression and cell behavior of recipient cells. For this reason, EVs are considered as signalosomes for several core biological processes in both physiological and pathological conditions[54].

EVs may activate immune responses or suppress inflammation in a tolerogenic manner, thereby participating in immune surveillance.

EVs confer immune suppression by several mechanisms: they can enhance the function of regulatory T cells, suppress natural killer (NK) and CD8+ cell activity, and inhibit monocyte differentiation into dendritic cell (DC) as well as DC maturation. By contrast, the effects of immune activation can be mediated by EV-promoted proliferation and survival of hematopoietic stem cells and the activation of monocytes, B cells and NK cells[55,56]. In blood circulation, EVs participate in the coagulation cascade by providing a surface for the assembly of clotting factors[57]. In addition, in the brain, neurons can communicate via the secretion of EVs, which contribute to local and distal synaptic plasticity[58].

EVs also take part in stem cell maintenance and plasticity, and they appear to have an essential role in the repair of injured tissue owing to their neoangiogenic, anti-apoptotic and cell proliferation-stimulating properties[59].

However, the same abilities of EVs that underline their important roles in the maintenance of normal physiology can also induce a worse clinical course in pathological conditions, such as in cancer progression and metastasis formation, in the generation and progression of neurodegenerative diseases, in cardiovascular diseases, as well as in infectious diseases[60].

EVs play decisive roles in cancer development by transferring oncogenes, regulating cancer-stroma interactions, developing the pre-

metastatic niche and encouraging angiogenesis. Moreover, tumor-derived exosomes (TDEs) and tumor microenvironment exosomes (TMEs) may carry pro-EMT (pro-epithelial-mesenchymal transition) cargoes that include EMT inducers, like TGF-β, β-catenin or miRNAs. All this content confers mesenchymal properties to epithelial cells and promotes the initial phase of tumor metastasis, when *in situ* tumor cells acquire the ability to migrate out of the primary tumor site, invading basement membrane and entering the circulatory system, and guarantees tumor-microenvironment crosstalk[61,62].

In infectious diseases, accumulating studies have shown that viruses could modulate their infection ability and pathogenicity through regulating the components and functions of EVs; in hepatitis C virus (HCV) infection, EVs are enriched in miRNAs targeting key components of immunoregulatory signaling pathways and antiviral interferon-mediated responses. Functionally, these structural EVs modifications lead to inhibition of NK cells degranulation; however, this effect is reverted after direct-acting antivirals (DAA) therapy[63].

Recently, Montaldo and collaborators demonstrated that EVs derived from plasma of HCV-infected patients display a profibrogenic ability on hepatic stellate cells, responsible for liver fibrosis, causing their transdifferentiation/activation. Structurally, these vesicles are enriched in pro-fibrogenic proteins and contain lower levels of antifibrogenic miRNAs compared to healthy donor EVs. Notably, also

in response to a sustained virological response due to a DAA therapy, the antifibrogenic cargo and the EVs activity remain unchanged[64].

1.5 Mechanisms for the selective loading of miRNAs into EVs

As discussed before, EVs include proteins, lipids, DNA, mRNAs, and noncoding RNAs. As important noncoding RNAs, miRNAs have attracted considerable attention, due to their regulatory roles in gene expression at the post-transcriptional level, and due to the observation that, among small RNAs, the proportion of miRNAs results to be higher in EVs than in their parental cells[65]. Generally, sorting mechanisms of miRNAs into EVs are classified as active or passive RNA-loading processes[66]. Passive loading into EVs strongly depends on the intracellular concentration of a certain miRNA, and its enrichment in EVs is exclusively source cell-conditioned[67,68]. On the other hand, the presence of an active, or selective, loading mechanism of miRNAs into EVs is indicated by an enrichment of a certain miRNA in EVs that is not necessarily mirrored in the overall miRNA content of the source cell[69,70]. Although the specific molecular mechanisms controlling this selective sorting of miRNAs into EVs are still poorly

understood, current research has highlighted several new insights about this biological process.

Neutral sphingomyelinase 2 (nSMase2) was the first reported molecule involved in miRNA sorting into EVs; some evidence shows that nSMase2 can regulate the content of miR-210 in exosomes derived from cancer cells and mesenchymal stem cells. nSMase2 can also regulate the entry of miR-10b into exosomes derived from metastatic breast cancer cells[71,72]. Moreover, inhibition of nSMase2 greatly reduces secretion of miR-16 and miR-146a within exosomes without any change in cellular miRNA levels. Likewise, overexpression of nSMase2 increases the abundance of miR-16 and miR-146a in exosomes with no effect on cellular miRNAs levels[73].

The vacuolar protein sorting-associated protein 4 (Vps4A) is required for normal endosomal trafficking and MVBs sorting but has also recently been implicated in cancer. In this regard, hepatocellular carcinoma cells (HCC) overexpressing Vps4A show elevated exosomal levels of miR-27b-3p and miR-92a-3p[74]. On the other hand, inhibition of Vps4A in HEK293 cells causes reduced levels of EV-loaded miR-92a and miR-150[75].

Currently, research has shown that KRAS oncogene form (wild-type or mutant) may influence the profile of miRNAs both in exosomes and their parental cells: for instance, miR-100 shows a higher expression level in mutant exosomes, while miR-10b is more highly expressed in

wild-type exosomes, and miR-320 families are enriched in both mutant and wild-type KRAS exosomes, suggesting that miR-320 families may be sorted into exosomes, regardless of the KRAS type[76].

New evidence indicates that Alix is also involved in miRNAs' loading into EVs; this has been specifically shown in human hepatic stem cell-like cells. Alix recruits the RNA-binding protein Ago2 to the endosomal membrane, which in turn induces miRNA binding and subsequent packaging into EVs[77].

Substance P (SP) and its receptor, NK1R, are implicated in the expression of many miRNAs in the cytosol of human colonocytes. Recently, SP/NK-1R signaling has also been shown to regulate the sorting of exosomal miRNAs; indeed, it was reported that the level of exosomal miR-21 produced by human colonocytes in response to SP signaling was increased compared to the levels of the same miRNA produced by unstimulated cells[78].

In addition, some sequence modifications of a miRNA itself can also determine its loading into EVs: the distribution of miRNA in human B cell-derived exosomes is related to the post-transcriptional modification of its 3′ end. Indeed the 3′ end adenylation facilitates miRNA retention in the cell, while 3′ end urine glycation may promote the inclusion of miRNA into exosomes[79]. Moreover, an increased post-transcriptional 3′-end uridylation of miR-2909 is the driving force for the recruitment of this miRNA to exosomes secreted by prostate

cancer cells (PC-3)[80]. Furthermore, adenosine kinase may be closely related to the addition of non-template nucleotides to the 3′ end of miRNAs, which has been observed in cancer cells, where it affects the distribution of miRNAs in the intracellular compartment and in cell-derived secreted exosomes. However, the role of adenosine kinase in the post-transcriptional modification of miRNAs and their subsequent sorting needs to be further explored.

1.5.1 RNA Binding Protein-Mediated EVs Loading

Among many EV-loading influencing factors, RNA-binding proteins (RBPs) seem the most important[81] (figure 5).

The argonaute2 (Ago2), a component of the RISC complex, is implicated in miRNA binding and sorting into EVs through the KRAS-MEK-ERK signaling pathway. Specifically, phosphorylated Ago2 impairs its localization into microvesicles (MVs) and decreases secretion into endosomes. Conversely, inhibition of MEK and ERK has been shown to decrease Ago2 phosphorylation and increase Ago2 accumulation inside exosomes. Thus, the miRNA sorting exerted by Ago2 appears to be controlled upstream by the KRAS-MEK-ERK pathway. Further, KRAS-MEK-ERK pathway-dependent phosphorylation of Ago2 has been demonstrated to exert some

specific control over the sorting of let-7a, miR-100, and miR-320a into exosomes[82]. Strengthening these findings, miR-100 levels within exosomes are elevated in oncogenic KRAS mutants with overactive phosphorylation[76]. Collectively, KRAS-MEK-ERK has a general regulatory ability over MVs and exosomal levels of Ago2, in addition to specific control over selected miRNAs.

Y-Box Binding Protein 1 (YBX-1) is another protein with RNA-binding domains and exerts a range of functions, including mRNA splicing and transport. YBX-1 has been found to regulate miR-133 packaging into exosomes after hyperoxia/reperfusion (H/R) treatment of endothelial progenitor cells (EPCs). Silencing YBX-1 through siRNA causes decreased miR-133 localization within H/R EPC-derived exosomes with no change of its expression in the EPC cytosol. Conversely, overexpression of YBX-1 with miR-133 mimics increases miR-133 quantity within H/R EPC-derived exosomes[83]. Additionally, it was found that YBX-1 is required to selectively package miR-223 into exosomes derived from HEK293T cells: YBX-1 promotion of miR-223 entry into exosomes does not depend on a specific recognition motif but proceeds through the interaction between its internal cold shock domain and miR-223[84].

MEX3C functions as an RNA-binding E3 ubiquitin ligase to assist with mRNA degradation. However, recent evidence has suggested that MEX3C could also play a role in miRNA sorting into EVs as

demonstrated by assays with siRNA molecules targeting MEX3C that cause a decreased exosomal level of miR-451a. Since no complementary sequences were found between MEX3C and miR-451a, Ago2, an interactor of MEX3C[85], might act as an intermediary between MEX3C and miR-451a. So, this MEX3C-Ago2 complex might transport miR-451a into exosomes[86].

Major vault protein (MVP), a ribonucleoprotein involved in transporting RNA from the nucleus to the cytoplasm, is a further regulator of miRNAs sorting into exosomes: indeed, MVP knockout in CT26 colon cancer cells causes increased cellular levels of miR-193a but decreases its loading within CT26-derived exosomes. This MVP knockout is miR-193a selective because there are no observed expression changes of another tested miRNA, the miR-126a[87].

The La protein is another RNA-binding protein that functions as a transcription factor for RNA polymerase III that shuttles between the nucleus and cytoplasm. Cytosolic La-depleted cells are associated with a 4-fold reduction of miR-122 sequestration into EVs[88].

1.5.2 Mechanisms for the selective loading of miRNAs into EVs depending on RBPs and sequence determinants

As mentioned above, the molecular players controlling the selective partition of miRNAs remain largely uncharacterized although recent evidence highlighted mechanisms of EV-loading depending on sequence-specific RNA-binding proteins (figure 5).

The hnRNPA1 protein, a ubiquitously expressed RNA-binding protein recognizing the UAGGG(A/U) motif, also mediates the sorting of miR-196a in EVs derived from cancer-associated fibroblasts (CAFs) through its binding to a specific motif (UAGGUA) at the 5′ end of miR-196a[89]. hnRNPA1 can promote also miR-522 entry into CAFs-derived exosomes after deubiquitination by USP7[90]. In addition to CAFs, hnRNPA1 can also promote the sorting of miR-320 for inclusion into EVs by recognizing specific motifs (AGAGGG) in leukemia cells[91].

SRSF1, originally identified as a splicing factor in eukaryotic cells, is also a shuttle between the nucleus and the cytoplasm to regulate RNA metabolism, miRNA processing and other cellular events independent of the mRNA splicing process. SRSF1 binds to miR-1246, the most abundant miRNA in exosomes derived from pancreatic cancer cells and its knockdown significantly reduces exosome miRNA enrichment for a majority of the selectively enriched exosome miRNAs, without altering the expression levels of less enriched

exosome miRNAs. A 6 bp miRNA motif commonly shared by the SRSF1-associated exosome miRNAs was also identified and this motif was demonstrated as specifically bound by SRSF1[92].

Villarroya and colleagues identified, in primary T-cells, two motifs significantly over-represented in miRNA specifically sorted in EVs (EXO motifs), and three motifs significantly over-represented in miRNA retained in cells (CL motifs), all of them significantly responsible for miRNA destiny. Most interesting, the conversion of the cell-retained miR-17 CL motif into an EXO motif resulted in a higher EVs loading while, in the complementary experiment, the conversion of the EXO motif in EV-loaded miR-601 into a CL motif resulted in a higher cell retention of this miRNA. By performing mass spectrometry, they also identified the heterogeneous nuclear ribonucleoprotein A2B1 (hnRNPA2B1) as a protein able to bind to miR-198 and miR-601, embedding the GGAC EXO-motif, and to guide their inclusion in EVs when SUMOylated[93].

Moreover, hnRNPA2B1 specifically recognizes the AGG/UAG motifs and strongly interacts with MVs-associated miR-17 and miR-93, which share these motifs. Additionally, it has been shown that Caveolin-1 (Cav-1) is integral in the trafficking process into MVs of hnRNPA2B1 and of hnRNPA2B1-associated miRNAs. In this regard, under cellular stress, an upregulation of Cav-1 localization occurs in MV membranes, that causes an increased release of hnRNPA2B1 into

MVs as well as elevated levels of hnRNPA2B1-associated miRNAs in MVs of hyperoxia-treated cells. Conversely, Cav-1 deletion causes a decrease of expression of hnRNPA2B1 in MVs in response to hyperoxia[94,95].

With the intent of characterizing further proteins responsible for miRNAs loading in EVs, Santangelo and collaborators characterized in hepatocytes, cellular and EVs-loaded microRNA repertoires, identifying a profile of EVs-enriched miRNAs, among which miR-3470a and miR-194-2-3p. Interestingly, a proteomic analysis by MALDI-TOF/TOF mass spectrometry (MS) on the protein pool associated with specific EV-miRNAs allowed to identify a new hnRNP, SYNCRIP (synaptotagmin-binding cytoplasmic RNA-interacting protein) as a specific miRNA interactor. Moreover, SYNCRIP was not associated with cytoplasmic miRNAs or other random sequences, suggesting a high level of specificity for the EVs-derived miRNAs. A deeper analysis disclosed that SYNCRIP can bind to EVs-enriched miRNAs sharing the common sequence GGCU, named hEXO-motif, that has a functional role in EVs miRNAs sorting. Indeed, the inclusion of the hEXO motif in miRNA-29b allowed SYNCRIP direct binding to this miRNA e increased this miRNA loading into EVs. Structurally, SYNCRIP binds to the hEXO motif through its N-terminal unit for RNA recognition (NURR) domain as

demonstrated through the removal of the NURR domain from SYNCRIP that impairs SYNCRIP binding to miR-3470.

SYNCRIP and hnRNPA2B1 display different sequence-specific EVs sorting capacities: hnRNPA2B1 binds to miRNAs with EXO motif and miRNAs with both EXO and hEXO motif, but not to miRs embedding only hEXO motif (e.g. miR-3470). Similarly, SYNCRIP doesn't bind to miRNAs with only GGAG EXO motif. Moreover, hnRNPA2B1 knockdown in hepatocytes does not cause a decrease in EVs loading of GGCU-containing miR-3470a and miR-194-2-3p, while the amount of miRNAs with the GGAG motif is reduced[96,97].

Recently, Garcia-Martin and colleagues showed that the miRNA population released in small EVs (sEVs) is clearly distinct from the population expressed in the cell of origin. Moreover, by using a robust system of five metabolically important cell types and miRNA profiling, they found that different miRNAs are enriched in sEVs depending on the cell type. By performing in silico sequence analysis, they identified, for each cell type, one to four motifs of 4–7 nucleotides, most with high G+C content, significantly associated with enrichment in sEVs, thus named EXO motifs. A similar analysis identified two to five motifs of 4–5 nucleotides in length in the cell-enriched miRNAs (CELL motifs) for each cell type, with low G+C content.

These sorting/retention motifs are sufficient to modify miRNA distribution between cells and sEVs since the introduction of the CELL

motif AGAAC into the sequence of the somewhat sEV-enriched miR-431-5p resulted in a decrease in its sEV loading while the mutation of the same AGAAC CELL motif in miR-140-3p, leads to doubling of its sEV export. On the other hand, EXO motif introduction into a highly cell-enriched miR-34c-5p, as well as for miR-26a, increases their sEV loading.

Moreover, by performing a mass spectrometry experiment, they identified two additional proteins, ALYREF and FUS, as interactors of miR-34c or miR-26a after the introduction of a CGGGAG EXO motif in the miRNA sequence. Finally, ALYREF and FUS knockdown results in a reduction of sEVs enrichment, demonstrating their involvement in miRNAs sorting.

Functionally, incorporation of EXO motifs enhances miRNA delivery from donor cell to recipient cells and, subsequently, the ability of the secreted miRNAs to inhibit target genes in recipient cells[98].

More recently, it has been demonstrated that also epitranscriptomics influences miRNAs extracellular compartmentalization: m6A modification, the addition of a methyl group to carbon 6 of adenosine (mediated by the METTL3/METTL14 complex) to miRNAs on RACH, RRACH, DRACH, and METTL3 motifs, impairs the interaction between the methylated miRNA fraction and AGO2 and, in turn, their function. Notably, the same modification enhances their extracellular delivery through the EV loader hnRNPA2B1 that preferentially

associates with methylated rather than with unmodified miRNAs. Thus, the hnRNPA2B1's ability to bind to miRNAs in a sequence-specific manner is extended to its ability to act as an m6A reader. Moreover, in recipient cell, methylated miRNAs delivered *via* EVs need a demethylation step mediated by the RNA demethylase FTO to rescue their function and act on their target mRNAs[99].

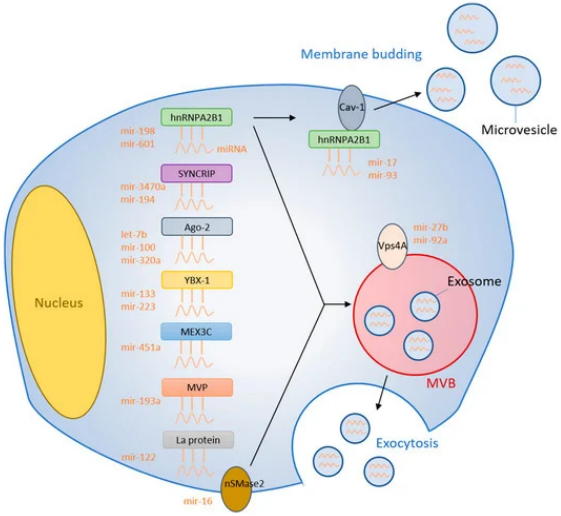

Figure 5. Summary of miRNA sorting into EVs
RNA binding proteins bind specific miRNAs and selectively shuttle them into EVs. Membranous proteins are also involved in the miRNA sorting mechanism
(From Groot M. et al Cells. 2020)

HETEROGENEOUS NUCLEAR RIBONUCLEOPROTEINS (hnRNPs)

Heterogeneous nuclear ribonucleoproteins (hnRNPs) are a highly evolutionarily conserved family of ubiquitously expressed RNA-binding proteins that share a wide array of nucleic acid targets as well as cellular and molecular functions. The hnRNP family encompasses over 20 proteins designated A through U, with varying molecular weights, ranging from 34 to 120 kDa, abundantly present in the nucleus and found in association with proteins to form hnRNP particles; they are able to translocate to the cytosol upon post-translational modification or by the recruitment of other hnRNPs[100].

The most important domains of hnRNP family proteins are represented by the RNA-binding motifs, which mediate general and specific interactions of the proteins with nucleic acids including RNAs and single-strand DNAs (ssDNA). In fact, there are different kinds of RNA-binding motifs in distinct hnRNPs and each hnRNP has one or more RNA-binding modules[101] (figure 6).

The most prevalent and highly conserved RNA-binding motif is the RNA recognition motif (RRM), which is approximately 90 amino acids long, forming a β1-α1-β2-β3-α2-β4 topology. The hallmark of the RRM is the presence of two highly conserved sequences referred to as

RNP1 and RNP2, which are separated by about 30 amino acids. RNP1 in the β3 strand and RNP2 in the β1 strand directly interact with RNA, resulting in the binding of RNA to the β sheet surface. In addition, the two external β sheets, the loops, and the C- and N-termini can promote the RNA-binding affinity and facilitate recognition for specific nucleotide sequences. The RRM modules are found in most of the hnRNPs, except for hnRNP K, E, and U, and are necessary and sufficient for RNA binding with high affinity and specificity[102].

The K homology (KH) domain, originally found in hnRNP K, is structurally different from the RRM and is characterized by a 45 amino acid repeat that can be split into two groups. The Type I KH domains have a βα extension in their C-terminus, whereas the Type II KH domains have an αβ extension in their N-terminus. The core region of the KH domain is characterized by three-stranded antiparallel β-sheets together with three α-helices (βααββα). Therefore, several copies of KH domains within a given protein are required for achieving greater RNA/ssDNA binding affinity and specificity[103]. In this frame, among all hnRNPs, the hnRNP K and hnRNP E1/E2 contain three KH domains that mediate the binding of hnRNPs to single-strand nucleic acids[104].

The RGG domain, which consists of several Arg-Gly-Gly (RGG) repeats interspersed with aromatic residues, is an arginine- and glycine-rich region that was discovered in some hnRNPs. RGG

repeats bind to RNA directly or indirectly through the association with other RNA-binding motifs. Moreover, dimethylation of arginine residues in the RGG box is common and represents an important modification in regulating RNA-binding activity. The RGG domain is alone or concomitant with other RNA binding modules in distinct hnRNPs: RGG repeats domain is the only RNA-binding domain identified in hnRNP U responsible for nucleic acid binding, while in hnRNP A1 RGG box coexists with RRMs and both of them function as nucleic acid binding domains[105].

Next to RNA-binding motifs, hnRNPs frequently contain auxiliary domains, such as proline-, glycine- or acid-rich domains: the modularity created by the combination of RNA-binding domains (RBDs) and auxiliary domains increases the functional diversity of hnRNPs[102].

The hnRNP proteins frequently undergo post-translational modifications, leading to changes in biological activity and subcellular localization. Reported post-translational modifications on hnRNPs include methylation, phosphorylation, ubiquitination and sumoylation[106].

In general, the functions of the hnRNPs in various cellular biological processes are based on their nucleic acid binding properties recognizing a wide range of RNA and ssDNA sequences, along with following formation of nucleotide-protein complexes that mediate

ssDNA or RNA processing. The hnRNPs assembling on DNA participate in DNA repair, chromatin remodeling, telomere maintenance, and gene transcription[107]. Meanwhile, the hnRNPs interacting with the RNA take part in every step of RNA metabolism including mRNA splicing, capping and polyadenylation, trafficking, translation, and turnover[108].

The expression levels of hnRNPs are altered in many types of cancer, suggesting their role in tumorigenesis. In addition to cancer, many hnRNPs were found to be associated with various neurodegenerative diseases, such as spinal muscular atrophy (SMA), amyotrophic lateral sclerosis (ALS), Alzheimer's disease (AD) and fronto-temporal lobe dementia (FTLD)[100].

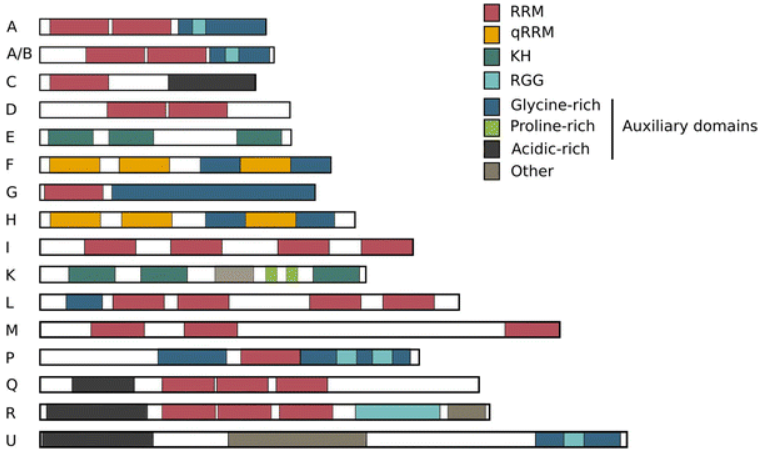

Figure 6. The hnRNP family
Structure of hnRNPs with multiple modules.
(From Geuens, T et al V.2016)

2.1 SYNCRIP: structure and functions

SYNCRIP, also named hnRNPQ, is an evolutionarily conserved hnRNP across eukaryotic organisms characterized by a molecular weight of 73 kDa. SYNCRIP exists in different splicing isoforms, three of which are the most representative: hnRNP Q3, hnRNP Q2, and hnRNP Q1.

SYNCRIP contains three conserved RRM domains flanked by a highly conserved N-terminal acidic domain reported to mediate the interaction with Apobec protein, and a long, unstructured, less conserved C-terminus, which has been reported to mediate the interaction with synaptotagmins and a G-quartet RNA[109-111]. Interaction between SYNCRIP and RNA targets is mediated not only by the three RRM domains but also by the N-terminal region that is joined to the RRM domains by an $\alpha\beta\beta$ motif, creating a continuous surface. This N-terminal domain named NURR (N-terminal unit for RNA recognition), as described previously, interacts with the hEXO motif mediating SYNCRIP-miRNA recognition, thus miRNA loading into EVs. Moreover, the NURR and RRM domains act together to achieve a specific and high-affinity interaction with the SYNCRIP RNA targets: the contacts between the NURR and RRM1 domains position the RRM domains 5′ of the NURR domain on the bound RNA sequence[97].

In addition to the role in miRNA EVs loading, SYNCRIP exerts different roles in the regulation of gene expression at the post-transcriptional and translational level, from pre-mRNA splicing and RNA editing to cytoplasmic mRNA transport for internal ribosome entry site (IRES)-mediated translational activation and mRNA degradation[112-114].

Due to its pleiotropic role, this protein is involved in several biological processes, such as neural and muscular development and homeostasis of hematopoietic stem and progenitor cells[115,116]. In the nervous system, for example, SYNCRIP takes part in the growth of neuromuscular junctions and in the nascent axons[111]. For this reason, dysfunctions of SYNCRIP are causative of different neuro-degenerative disorders and cardiomyopathies[114].

SYNCRIP is also involved in several types of cancer: in acute myeloid leukemia, SYNCRIP interacts with the RBP MSI2, which is a central regulator of cancer stem cell fate[117]; in colorectal cancer SYNCRIP guarantees cellular proliferation through the formation of a complex with Galectin-3 that stabilizes SYNCRIP[118]. In HCC, SYNCRIP is an important prognostic marker: high expression level of this protein positively correlates with a negative prognosis (as reported in the Human Protein Atlas, https://www.proteinatlas.org).

More recently, an additional role for the RNA binding protein SYNCRIP has been described in the modulation of EMT/MET

(epithelial to mesenchymal transition/ mesenchymal to epithelial transition) dynamics in liver, in which the involvement of transcription factors and ncRNAs has already been described[119-124]: SYNCRIP, in hepatocytes, acts as a "mesenchymal" gene, being induced by TGFβ and positively modulating the EMT. Indeed, SYNCRIP silencing limits the induction of the mesenchymal program and maintains the epithelial phenotype. In HCC invasive cells, SYNCRIP knockdown induces a mesenchymal–epithelial transition (MET), negatively regulating their mesenchymal phenotype and significantly impairing their migratory capacity. Moreover, during EMT/MET dynamics, SYNCRIP knockdown impacts the expression of a set of miRNAs with pro- or anti-EMT properties, suggesting the possible involvement of this RNA binding protein in their transcriptional regulation[125].

2.2 PCBP2: structure and functions

Poly(rC)-binding protein 2 (PCBP2), also named hnRNPE2, is an RNA-binding protein able to interact with the poly(C) in a sequence-specific manner and with high affinity. PCBP2 is part of PCBPs family including PCBP1, PCBP3, PCBP4 and hnRNP K, characterized by the presence of KH-domains[104] (figure 7A). PCBP2 contains three KH

domains which are separated by variable length insert sequences; the structure of each KH domain consists of three α-helices and an antiparallel β-sheet that fold according to a $\beta1\alpha1\alpha2\beta2\beta3\alpha3$ motif. The KH domain is the consensus RNA-binding domain and recognizes and combines with RNA, C-rich regions of ssDNA, and dsDNA. PCBP2 KH1 domains can dimerize on exposed surfaces opposite from nucleotide-binding sites, PCBP2 KH2 domain folds might be similar to that of KH1 and PCBP2 KH3 may also interact with the same nucleotide sequence but it is unable to dimerize[126,127]. Moreover, PCBP2 has two types of nuclear localization signal (NLS) sequences that are responsible for transporting proteins from the cytoplasm to the nucleus: NLS1 is located between the KH2 and KH3 domains, and NLS2 is located on the KH3 domain. PCBP2 is predominantly localized to the nucleus but the PCBP2 splice variant and PCBP2-KL are localized both in the nucleus and in the cytoplasm[128].

Due to its affinity for the Poly(C), PCBP2 can bind to the promoters of multiple genes to regulate gene transcription: PCBP2 specifically binds to a specific region on the promoter of hereditary breast cancer susceptibility gene (BRCA1) to regulate BRCA1 transcription[129] (figure 7B).

At the post-transcriptional level, PCBP2 can bind with high affinity, through its KH domains, to the pyrimidine-rich 3'untranslated region (3'UTR) of collage α-globin mRNA with a consequent increase in

mRNA stability (figure 7C). PCBP2 is also constituent of a stabilizing complex on the UTR of the β-globin mRNA that exhibits many of the properties of the α-complex[130]. On the contrary, PCBP2 negatively regulates and suppresses the expression of the mRNA for the G protein-coupled receptor 56 (GPR56), which modulates mechanical overload-induced muscle hypertrophy. In this regard, PCBP2 enhances GPR56 mRNA degeneration in cardiomyocytes, thus serving as an anti-hypertrophic factor[131].

PCBP2 is known to bind to mRNAs, exerting regulatory activity at the translational level (figure 7D); indeed, it can increase c-Myc internal ribosome entry site (IRES) activity by specifically binding to the c-Myc mRNA IRES *in vivo* and *in vitro*[132]. PCBP2 also interacts with the main stem-loop IV structure of the poliovirus IRES and is required for effective translation of poliovirus RNA in HeLa cells[133].

In recent years, PCBP2 has been reported to participate in iron metabolism by acting as a molecular chaperone for iron to enter ferritin and forming a stable complex with it[134].

PCBP2 has also been found to bind to the iron (Fe [II]) channel protein divalent metal transporter 1 (DMT1) to regulate the ability of DMT1 to transport iron; knockout of PCBP2 or DMT1 leads to a decrease in iron uptake in cells, and PCBP2 can bind to Fe (II) transporter (ferroportin) to regulate Fe (II) transmembrane transportation. Thus, PCBP2 works as a "gateway keeper" for transmembrane iron

transport. Furthermore, PCBP2 can deliver Fe (II) to deoxyhypusine hydroxylase (DOHH) to regulate the activity of prosthetic iron-containing enzymes in cells. Silencing of PCBP2 leads to changes in the structure of intracellular DOHH and loss of activity *in vitro*[135].

PCBP2 plays a central role also in several human cancers; high PCBP2 expression is associated with poor prognosis and was found to improve HCC cell proliferation and to promote therapy resistance in HCC cells[136]. Mechanistically, PCBP2 oncogenic activity is mediated by interaction with Yes-associated protein (YAP), necessary for tumour growth[137].

PCBP2 expression is also highly expressed in advanced stages of glioblastoma and is associated with higher histological grade, clinical stage, and poorer prognosis[138]. Moreover, PCBP2 functions as a tumour promoter in facilitating glioma cell proliferation, migration, invasion, and EMT, while inhibiting apoptosis[139,140].

Also, in gastric carcinoma, the up-regulation of PCBP2 levels was associated with high disease grade, poor postoperative relapse-free survival, and poor overall survival rates of gastric cancer patients. In this context, lncRNA ST8SIA6-AS1 and lncRNA KCNQ1OT1 could upregulate PCBP2 expression by sponging miR-5195 and miR-145-5p, respectively, thereby promoting cancer progression through PCBP2 that can facilitate cancer cell proliferation, invasion, migration and

inhibit apoptosis by directly binding to miR-34a, typically downregulated in this type of cancer[76,141].

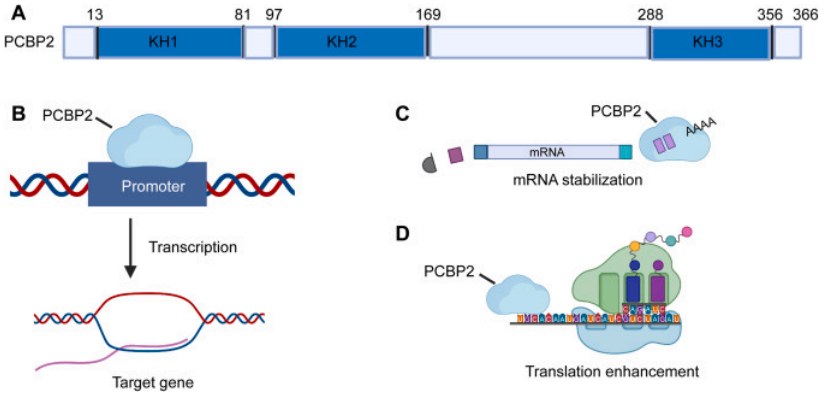

Figure 7. The structure and molecular function of PCBP2 protein
(A) Multi-domain structure of PCBP2 protein. (B–D) PCBP2 performs multiple functions, including transcription, mRNA stabilization, and translation enhancement.
(From Yuan C et al. Biomed Pharmacother. 2021)

AIM OF THE WORK

Extracellular vesicles (EVs) are important mediators of intercellular communication by transferring their specific informational cargo (e.g. nucleic acids, proteins, metabolites) from a producing to a receiving cell. The EVs cargo is defined by dynamic and selective cell-specific loading mechanisms. With respect to ncRNAs, and specifically to miRNAs, the molecular players controlling their selective delivery into EVs remain largely uncharacterized. In particular, sequence determinants causing miRNAs export (EXO motifs) or intracellular retention (CELL motifs) have been identified; however, while for EXO motifs different RNA-binding proteins have been characterized as able to directly bind to these sequences and to promote miRNA export, for the CELL motifs the identification of interacting proteins remains unaddressed.

Based on this body of evidence, the aim of this work was the biochemical and functional characterization of molecular players involved in the recognition of specific CELL motifs and responsible for miRNAs intracellular retention in dependence on these consensus sequences. It has also been explored the balance between RBPs-dependent miRNAs' EV-sorting and intracellular retention.

Based on literature evidence and on obtained data, we pursued the goal to shed light on multiprotein machineries that dynamically govern miRNAs' destiny. This was achieved by initially focusing on specific miRNAs and then by extending the observation to a broader repertoire of miRNAs to confirm that the observed mechanism had a general relevance.

In perspective, the knowledge on the molecular players defining miRNAs intracellular/EVs partition could be instrumental for the development of RNA-based manipulations of EVs cargo that could have a substantial impact on intercellular communication for therapeutic purposes.

MATERIALS AND METHODS

Cell culture conditions

Nontumorigenic murine hepatocyte 3A cells[64,142] were grown at 37°C, in a humidified atmosphere with 5% CO2, in RPMI 1640 medium (Gibco; Life Technologies) supplemented with 10% fetal bovine serum (FBS; Gibco-Life Technology), 50 ng/mL epidermal growth factor (EGF; PeproTech Inc.), 30 ng/mL insulin growth factor (IGF) II (PeproTech Inc.), 10 mg/mL insulin (Roche Applied Science), and penicillin/streptomycin, on dishes coated with collagen I (Collagen I, Rat Tail; Gibco Life Technology).

Extracellular vesicle purification

Extracellular vesicles were prepared according to International Society of Extracellular Vesicles (ISEV) recommendations[9]. Conditioned media (CM) from 150 mm plates, each containing 250.000 hepatocytes, were collected after 72 hours of culture in complete medium containing EVs-depleted FBS. Cell-conditioned media were centrifuged at 2.000 g for 20 minutes at 4°C to remove dead cells and then at 20.000 g for 30 minutes at 4°C. Cleared supernatants were

passed through 0.22 μm filter membranes, ultracentrifuged in a SW32 Ti rotor (Beckman Coulter) at 100.000g for 70 minutes at 4°C, and finally resuspended in PBS. The EVs resuspension was analyzed by Tunable Resistive Pulse Sensing (TRPS) technology using EXOID-V1-SC (Izon Science) for size and concentration characterization.

Biotin miRNA pull-down

Biotin miRNA pull-down experiments were performed on cytoplasmic extracts. Briefly, cells were lysed in hypotonic buffer (10 mM Tris-Cl [pH 7.5], 20 mM KCl, 1.5 mM MgCl2, 5 mM DTT, 0.5 mM EGTA, 5% glycerol, 0.5% NP-40, and 40 U/mL RNAsin [Promega Corporation, Madison, WI, USA]) supplemented with protease inhibitors (Roche Applied Science). Lysates were incubated on a rotating platform for 30 minutes at 4°C and then centrifuged at 13.000 rpm for 30 minutes at 4°C. Protein concentration was determined with Protein Assay Dye Reagent (Bio-Rad Laboratories Inc., USA) based on the Bradford assay.

Samples (2 mg of proteins) were incubated for 1 hour at 4°C with 10 nmol synthetic single-strand miRNA oligonucleotides containing a biotin modification attached to the 5′ and via a spacer arm (IDT, Integrated DNA Technology) (Table 1). Dynabeads™ M-280 Streptavidin (50 μl/sample, Invitrogen™), previously blocked with 1

mg/mL yeast tRNA (Roche Applied Science), were added to the reaction mixture for 90 minutes at 4°C, and then the beads were washed three times with cold lysis buffer and once with PBS. Elution was performed at room temperature for 5 minutes in Laemmli Buffer (containing 2-β mercaptoethanol and SDS).

Detection of miRNA/RBPs interaction was evaluated by WB on 10% of input sample and 50% of the pulled-down samples.

RNA pull-down assay with PCBP2 (NM_001103165) mouse recombinant protein (TP522190, Origene) was performed with 4 μg of protein.

Name	**Oligonucleotide sequence**
Biotin-miR-26b-3p WT	[Btn] 5′ CCUGUUCUCCAUUACUUGGCUC 3′
Biotin-miR-26b-3p no-hEXO	[Btn] 5′ CCUGUUCUCCAUUACUUGGCGA 3′
Biotin-miR-31-3p WT	[Btn] 5′ UGCUAUGCCAACAUAUUGCCAUC 3′
Biotin-miR-31-3p + hEXO	[Btn] 5′ UGCUAUGCCAACAUAUUGGGCUG 3′
Biotin-miR-31-3p +hEXO no-CELL	[Btn] 5′ UGCUAUGCCAACAUAUUUGGCUG 3′
Biotin-miR-155b-3p WT	[Btn] 5′ CUCCUACCUGUUAGCAUUAAC 3′
Biotin-miR-155b-3p no-CELL	[Btn] 5′ CUCCUACCUGUUAGCAUGAUC 3′
Biotin-miR-155b-3p no-hEXO	[Btn] 5′ CUCCUACCUGUUAGCAUUAGU 3′
Biotin-miR-365-2-5p WT	[Btn] 5′ AGGGACUUUCAGGGGCAGCUGUG 3′

Table 1. Biotinylated RNA oligonucleotides used in pull-down experiments

Protein digestion, peptide purification and nanoLC analysis

Proteins obtained from the pull-down experiments with miR-155-3p or random scrambled miRNA were separated on 4-12% gradient gels (Invitrogen™) and stained by Simply Blue Safe Stain staining. Fourteen sections of the gel lane were cut. Protein digestion of gel pieces and peptide purification were performed as previously described in [143]. Peptides resuspended in a suitable nanoLC injection volume of 2.5% ACN/0.1% TFA and 0.1% formic acid were then analyzed by an UltiMate 3000 RSLCnano-LC system, (Thermo Fisher Scientific) connected on-line via a nano-ESI source to an Q Exactive plus™ Hybrid Quadrupole-Orbitrap™ Mass Spectrometer (Thermo Fisher Scientific) as in [64]. Proteins were automatically identified by MaxQuant (v. 1.6.17.0) software. Tandem mass spectra were searched against the *Mus Musculus* dataset of UniprotKB database.

Quantitative comparison among miR-155-3p WT and miR-155-3p no-CELL was performed using the label-free quantification algorithm calculated by MaxQuant software.

SDS-PAGE and western blotting

Cells were lysed in Triton 1X Buffer, subsequently the proteins were analyzed as in[124]. The following primary antibodies were used for immunoblotting: α-PCBP2 (AV40568 – Sigma Aldrich), α-SYNCRIP (MAB11004 – Merck Millipore), α-HSP90 (sc-13119 – Santa Cruz Biotech.), α-LAMP1 (ab24170 – Abcam), α-CD63 (sc-5275 – Santa Cruz Biotechnology), α-SYNTHENIN (ab133267 – Abcam) α-CALNEXIN (NB100-1965 – Novus Biologicals), α-GAPDH (MAB-374 – Merck Millipore) used as a loading control. The immune complexes were detected with horseradish peroxidase-conjugated species-specific secondary antiserum (*α*-Rabbit 172-1019 and *α*-Mouse 170-6516; Bio-Rad Laboratories Inc., USA), then by enhanced chemiluminescence reaction (Bio-Rad Laboratories Inc., USA). Densitometric analysis of protein expression was performed by using the Fiji-Image J image processing package.

RNA extraction, RT-PCR and Real-Time qPCR

miRNAs were extracted by miRNeasy Mini Kit and RNeasy MinElute Cleanup Kit (QIAGEN), and reverse transcribed with MystiCq® microRNA cDNA Synthesis Mix (Sigma-Aldrich). Quantitative polymerase chain reaction (RT-qPCR) analyses were performed

according to MIQE guidelines. cDNAs were amplified by qPCR reaction using GoTaq qPCR Master Mix (Promega Corporation, Madison, WI, USA). Relative amounts, obtained with 2^(-ΔCt) method, were normalized with respect to the cel-miR-39 Spike-In (59000; NORGEN), previously added into miRNA samples.

Total RNA was extracted by ReliaPrep™ RNA Tissue Miniprep System (Promega Corporation, Madison, WI, USA) and reverse transcribed with iScriptTM c-DNA Synthesis Kit (Bio-Rad Laboratories Inc., USA). Quantitative polymerase chain reaction (RT-qPCR) analyses were performed according to MIQE guidelines. cDNAs were amplified by qPCR reaction using GoTaq qPCR Master Mix (Promega Corporation, Madison, WI, USA). Relative amounts, obtained with 2^(-ΔCt) method, were normalized with respect to the housekeeping gene 18S. Oligonucleotide sequences are reported in Table 3.

The results were analyzed with Manager Software (Bio-Rad Laboratories Inc., USA) and calculated by the ΔC(t) method.

miRNA	Primer sequence
mmu-miR-23a-5p	GGGGTTCCTGGGGATGGGATTT
mmu-miR-26b-3p	CCTGTTCTCCATTACTTGGCTC
mmu-miR-31-3p	TGCTATGCCAACATATTGCCATC
mmu-miR-122b-3p	AAACACCATTGTCACACTCCAC
mmu-miR-155- 3p	CTCCTACCTGTTAGCATTAAC
mmu-miR-155-5p	TTAATGCTAATTGTGATAGGGGT
mmu-miR-181d-5p	AACATTCATTGTTGTCGGTGGGT
mmu-miR-192-5p	CTGACCTATGAATTGACAGCC
mmu-miR-214-3p	ACAGCAGGCACAGACAGGCAGT
mmu-miR-345-3p	CCCTGAACTAGGGGTCTGGAGAC
mmu-miR-365-2-5p	GACTTTCAGGGGCAGCTG
mmu-miR-3084-5p	GTTGAAGGTTAATTAGCAGAGT

Table 2. Primers for miRNA qPCR analysis

Name	Primer sequence
PCBP2	*For* ACACCGGATTCAGTGGCA *Rev* TTGATTTTGGCGCCTTGACG
SYNCRIP	*For* ACCTTGCCAACACGTAACA *Rev* CCATAGCCTTGACACACCA
18S	*For* AGCACCCATTGCAACGTCTG *Rev* GCACGGCGACTACCATCG

Table 3. Primers for gene expression qPCR analysis.

Co-Immunoprecipitation (co-IP)

Cells were lysed with IP Lysis Buffer (150 mM NaCl, 50 mM Tris-HCl pH 7.5, 5mM EGTA pH 8, 50 mM NaF pH 8, 1.5 mM MgCl2, 1% TRITON-X100 and 10% glycerol) containing freshly added cocktail protease inhibitors (complete EDTA-free Protease Inhibitor Cocktail; Sigma Aldrich) and phosphatase inhibitors (5 mM EGTA pH 8.0; 50 mM sodium fluoride; 5 mM sodium orthovanadate). Lysates were incubated on a rotating platform for 2 hours at 4°C and then centrifuged at 13.000 rpm for 30 minutes at 4°C. Protein concentration was determined with Protein Assay Dye Reagent (Bio-Rad Laboratories Inc., USA), based on the Bradford assay.

2 mg of proteins (one for the specific antibody and one for the corresponding non-specific IgG) were precleared by adding 40 μL of Protein A Sepharose or Protein G Sepharose (GE HealthCare) for 3 hours at 4°C in a total volume of 1 ml of IP Lysis Buffer in rotation. Then, Protein A or G Sepharose was removed by centrifugation and the extracts were incubated with 5 μg of specific antibody α-PCBP2 (cod. RN025P – MBL), α-SYNCRIP (MAB11004 – Merck Millipore), Normal Rabbit IgG (12-370 – Merck Millipore) or Normal Mouse IgG (12-371 – Merck Millipore), the last two used as negative controls, to proceed with immunoprecipitation at 4°C overnight. Immuno-complexes were collected adding 50 μL of Protein A or G Sepharose

for 3 hours at 4°C in rotation. The immunoprecipitated proteins were washed three times with Net Gel Buffer (150 mM NaCl, 50 mM Tris-HCl pH 7.5, 1mM EDTA, 0.1% NP40 and 0.25% gelatin) and once with RIPA Buffer (150 mM NaCl, 1% NP40, 0.5% Sodium Deoxycholate, 0.1% SDS, 50 mM Tris HCl pH 8). Finally, immunoprecipitated proteins were detached from Sepharose beads by adding 50 μL of Laemmli Buffer 2X. Samples were boiled at 95°C for 5 minutes, beads were eliminated by centrifugation and 10% of input sample and 50% of each immunoprecipitated sample were loaded on polyacrylamide gel and analyzed by Western Blotting.

RNA Electrophoretic mobility shift assay (EMSA)

Cells were lysed in Triton Buffer at 4°C, for 30 minutes and 4 μg of protein extract were incubated with 0.5 pmol of biotinylated RNA oligonucleotides for 30 minutes at room temperature in REMSA Binding Buffer, according to the manufacturer's protocol (20158; Light Shift Chemiluminescent RNA EMSA Kit, Thermo Fisher Scientific). 1 μg of each antibody was incubated with the protein-RNA complex: anti-PCBP2 (RN025P – MBL), anti-SYNCRIP (MAB11004 – Merck Millipore) for supershift and ultrashift analysis. The electrophoresis was performed in native 6% polyacrylamide gel in 0.5X TBE. Transfer

step was carried out at 25V, for 15 minutes in 0.5X TBE and the detection was performed following the manufacturer's instructions.

UV cross-linking RNA immunoprecipitation (RIP)

UV cross-linking RIP was performed as reported in [124]. Immunoprecipitated miRNAs were reverse transcribed and analyzed by RT-qPCR amplifications. List of primers is reported in Table 2. Primary antibodies for IP: α-PCBP2 (RN025P – MBL), α-SYNCRIP (MAB11004 – Merck Millipore) and as negative controls Normal Rabbit IgG (12-370 – Merck Millipore) or Normal Mouse IgG (12-371 – Merck Millipore).

Gene silencing

Stable PCBP2 knockdown was achieved through infection with shRNAs cloned in pSUPER retro puro retroviral vector (Oligoengine). Viral supernatants were collected 48 hours after transfection of 293gp packaging cells, filtered (0.45 μm), and added to hepatocytes. At 48 hours post-infection, selection was performed with 2 μg/mL puromycin for at least 1 week before analysis. The sequence of shRNA

scramble used as control was previously described[144]. The sequences of shRNA oligos used for cloning are reported in Table 4.

Name	Sequence
PCBP2	*Sense* GATCCCCGAGCAGACCCATCCATAATTTCAAGAGAAT TATGGATGGGTCTGCTCTTTTTA *Antisense* AGCTTAAAAAGAGCAGACCCATCCATAATTCTCTTGA AATTATGGATGGGTCTGCTCGGG
SYNCRIP	As reported in[96].
CTR	As reported in[96].

Table 4. Oligos for shRNA cloning in pSUPER.retro.puro vector

Motif scanning analysis

Murine mature miRNA sequences were retrieved from miRBase v22.1 database[145]. The FIMO tool[146] was used to scan these sequences for occurrences of hEXO, extended CELL and core AUUA/G CELL motifs, encoded as Position Probability Matrices, with parameters --bfile --motif-- --norc and setting the p-value threshold to 0.1, 0.1 and 0.01, respectively. Motif instances falling in the seed regions (nucleotides 2-7) were ignored.

Small RNA sequencing

miRNA samples (two biological replicates per condition), to which the cel-miR-39 Spike-In (59000; NORGEN) was previously added, were sequenced at Procomcure Biotech GmbH. Sequencing libraries were prepared using the NEXTFLEX Small RNA-Seq Kit v4 (PerkinElmer). The sequencing reaction was performed on a Illumina NovaSeq 6000 instrument in 2x40bp paired-end configuration, with a throughput of ~40 million read pairs per sample. FastqToolkit version 2.2.5 (available at https://www.illumina.com/products/by-type/informatics-products/basespace-sequence-hub/apps/fastq-toolkit.html) was used to remove adapter sequences from the 3' end and to filter out reads whose length and average quality after trimming were < 10 and < 30, respectively. Only forward reads were kept for downstream analyses. The mirPRo software version 1.1.4 [147] which utilizes NovoAlign[148] as its alignment engine, was used to align reads to a reference composed of miRNA hairpin sequences downloaded from miRBase v22.1 database with the addition of the spike-in, and to count reads mapping to mature miRNAs. A count matrix was assembled, including only mature miRNAs with one or more reads in at least two cell and two EV samples. Differential abundance analysis was performed using the DESeq2 R package[149]. Size factors were estimated directly from spike-in counts. For each mature miRNA, a likelihood

ratio test was conducted to assess differences between the EV/cell abundance ratios measured in the shPCBP2 and shCTR conditions.

Statistical analyses

For the qRT-PCR analysis, statistical differences were assessed with the one-tailed paired Student's t-test using GraphPad Prism Version 9 (GraphPad Software). Data are presented as mean ± SEM, and p values < 0.05 were considered statistically significant. For the statistical analysis of proteomic studies, Perseus software (version 1.6.7.0) after log2 transformation of the intensity data was used. Results were considered statistically significant at $p<0.05$.

Data availability

The miRNA-seq data generated in this study have been deposited and are available in the GEO database under accession code GSE269709.

RESULTS

1. PCBP2 recognizes a CELL motif and has a functional role in intracellular retention of miRNA-155-3p

Aiming to identify RNA-binding proteins involved in miRNAs' intracellular retention, proteins from murine non-tumorigenic 3A hepatocytes were used in RNA pull-down experiments coupled to mass spectrometry by using as specific bait the miRNA-155-3p, selected for the presence of the CELL-motif identified in AML12 cells[98] (figure 1A).

Label-free nano-liquid chromatography mass spectrometry proteomic analysis (nLC-MS/MS) allowed to identify miR-155-3p-interacting proteins and label-free quantification intensities analysis identified 21 proteins enriched in miR-155-3p pull-down with respect to miR-155-3p mutated in the CELL motif (miR-155-3p no-CELL) (figure 1A-B): twelve of them are classified as RNA-binding proteins, with six containing at least one canonical RNA-binding domain[150-153] (figure 1C). For three of them, RNA-binding preferences are also known (i.e. PCBP2 prefers CU-rich sequences[152,154], LARP1 recognizes the CAP

and the 5′ top motif in mRNAs[155] and STAU1 binds to double-stranded RNAs[156].

A

miR-155-3p WT
CUCCUACCUGUUAGCAUUAAC
miR-155-3p no-CELL
CUCCUACCUGUUAGCAUGAUC

B

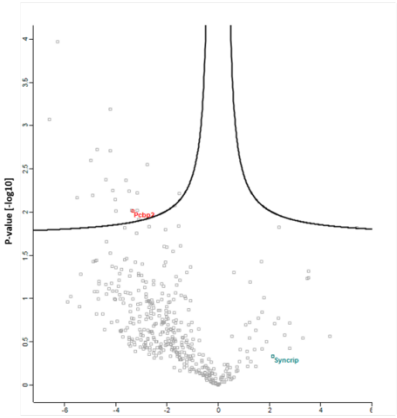

C

Protein names	Gene names	RBP Type	RNA Binding domain(s)
60S ribosomal protein L32	Rpl32	Canonical_RBP	|Ribosomal_L14|
Calponin;Calponin-2	Cnn2	No RBP	N.A.
Hydroxymethylglutaryl-CoA synthase, cytoplasmic	Hmgcs1	No RBP	N.A.
NEDD8-conjugating enzyme Ubc12	Ube2m	No RBP	N.A.
Fructose-bisphosphate aldolase;Fructose-bisphosphate aldolase A	Aldoa	Non-canonical_RBP	N.A.
Sorting nexin-3	Snx3	No RBP	N.A.
Zinc finger C2HC domain-containing protein 1A	Zc2hc1a	No RBP	N.A.
Protein disulfide-isomerase	P4hb	Non-canonical_RBP	N.A.
	Serpinb9b	No RBP	N.A.
Nascent polypeptide-associated complex subunit alpha	Naca	Non-canonical_RBP	N.A.
Copine-1	Cpne1	Canonical_RBPs	|RRM1|
La-related protein 1	Larp1	Canonical_RBPs	|La|
Bifunctional lysine-specific demethylase and histidyl-hydroxylase MINA	Mina	No RBP	N.A.
Cell growth-regulating nucleolar protein	Lyar	Non-canonical_RBP	N.A.
Replication factor C subunit 3	Rfc3	No RBP	N.A.
Poly(rC)-binding protein 2	**Pcbp2**	**Canonical_RBP**	**|KH_2|KH_1|**
Double-stranded RNA-binding protein Staufen homolog 1	Stau1	Canonical_RBP	|dsrm|Staufen_C|
Tumor susceptibility gene 101 protein	Tsg101	No RBP	N.A.
Zinc finger CCCH domain-containing protein 15	Zc3h15	Canonical_RBPs	|zf-CCCH|zf-CCCH_2|
p21-activated protein kinase-interacting protein 1	Pak1ip1	No RBP	N.A.
T-complex protein 1 subunit delta	Cct4	Non-canonical_RBP	N.A.

Figure 1. Proteomic identification of CELL-motif dependent miR-155-3p interactors

A) Sequences of biotinylated oligos used as bait in RNA pull-down experiment: miR-155-3p WT and miR-155-3p devoid of CELL motif (no-CELL). CELL motifs (WT and mutated) are in grey, hEXO motif is underlined.

B) Volcano plot comparing proteins bound to miRNA-155-3p no-CELL vs WT. Black curves represent the significant threshold at a false-discovery rate (FDR) of 0.05 and S0 of 0.1. PCBP2 and SYNCRIP proteins are labelled in the plot.
C) Results of proteomic analysis of proteins differentially bound to miRNA-155-3p no-CELL vs WT.

Among these proteins, PCBP2 interaction with miR-155-3p was confirmed by RIP assay (figure 2A, left panel) and RNA pull-down followed by western blot analysis (figure 2B).

Second evidence for the requirement of PCBP2/CELL motif interaction is provided by the observation on the CELL motif-devoid miR-365-2-5p that does not interact with PCBP2 (figure 2A, middle panel); RNA pull-down confirmed the absence of this interaction (figure 2C). In order to evaluate if PCBP2 binding was direct, we also performed an RNA pull-down using a PCBP2 recombinant form: in line with the previous results, the introduction of a specific mutation in the miR-155-3p CELL-motif impairs PCBP2 binding (figure 2D), further confirming the sequence specificity of this interaction and demonstrating that, at least *in vitro*, this binding is direct.

The miR-155-3p sequence embeds also an hEXO motif, a previously identified SYNCRIP binding site: RIP assay (figure 2E) confirmed SYNCRIP binding to this miRNA. Moreover, MS/MS analysis (figure 1B) and RNA pull-down followed by western blot analysis (figure 2B) demonstrated that this interaction occurs independently of the CELL motif mutation. Surprisingly, the introduction of a specific mutation

in the SYNCRIP-binding motif (miR-155-3p no-hEXO) impairs not only SYNCRIP binding, as expected, but also PCBP2 binding despite the conservation of the CELL retention motif (figure 2B). These data suggest a possible SYNCRIP requirement for PCBP2 binding. To test this hypothesis, RIP assay was performed on miR-31-3p, embedding the sole CELL motif: as reported, in the absence of the hEXO motif, PCBP2 is not able to bind this miRNA (figure 2A, right panel).

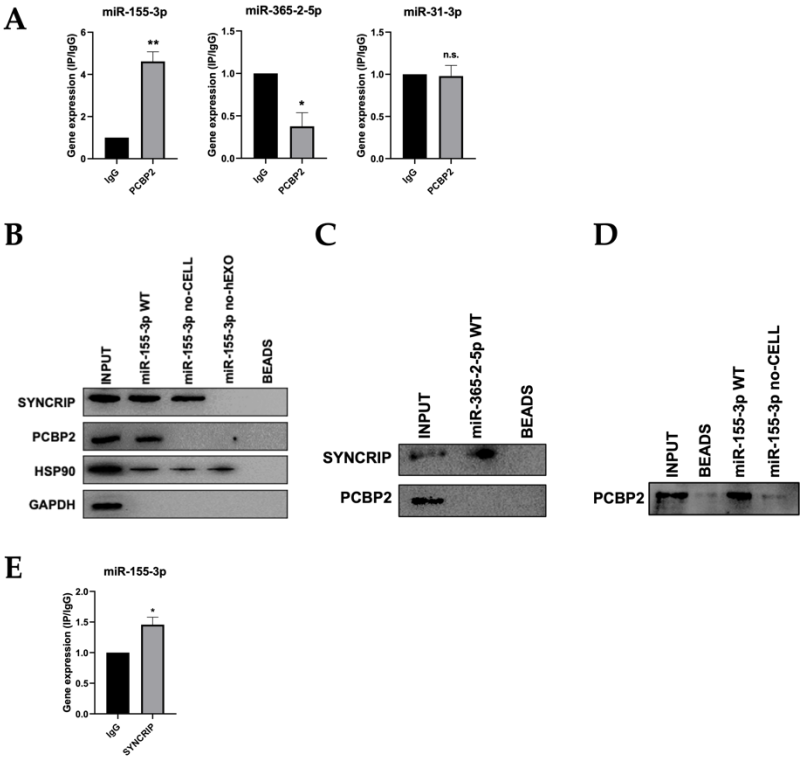

Figure 2. PCBP2 recognizes the CELL motif but requires also the hEXO motif

A) UV-crosslinking RIP of PCBP2 protein in murine hepatocytes. RT-qPCR analysis for miR-155-3p, miR-365-2-5p (CELL motif-devoid) and miR-31-3p (hEXO motif-devoid) is shown as IP/IgG. Data are the mean ± SEM of three independent experiments.
B) RNA pull-down with the WT and mutated (no-CELL, no-hEXO) miR-155-3p followed by western blot for the indicated proteins (HSP90 is used as positive and GAPDH as negative controls respectively). Data are representative of three independent experiments.
C) RNA pull-down with miR-365-2-5p followed by western blot for the indicated proteins. Data are representative of three independent experiments.
D) RNA pull-down by using the recombinant PCBP2 protein and with WT and mutated miR-155-3p (no-CELL) followed by western blot for PCBP2. Data are representative of three independent experiments.
E) UV-crosslinking RIP of SYNCRIP protein in murine hepatocytes. RT-qPCR analysis for miR-155-3p is shown as IP/IgG. Data are the mean ± SEM of three independent experiments.

In order to clarify a possible role for PCBP2 in miRNA intracellular retention, the effect of PCBP2 silencing on miRNAs' partition between cell and extracellular vesicles was evaluated. In brief, hepatocytes were infected with retroviruses expressing a short hairpin RNA silencing PCBP2, or a scrambled sequence as control, and 48 hours post-infection, stable 3A shCTR and shPCBP2 cell lines were obtained upon a selection step with 2 μg/mL puromycin for 1 week. Figure 3A-B shows the significant reduction of PCBP2 mRNA and protein

expression levels in shPCBP2 hepatocytes compared to control cells.

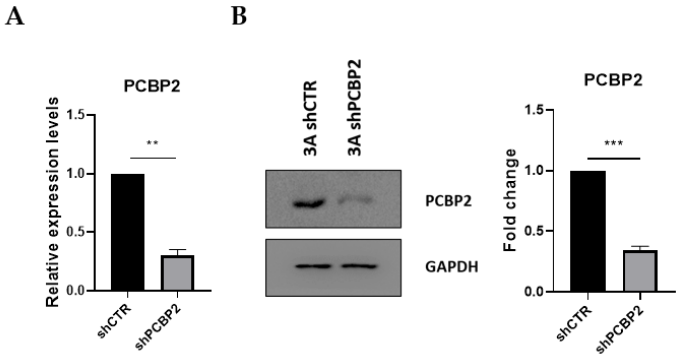

Figure 3. PCBP2 silencing

A) Expression levels of pcbp2 in shCTR and shPCBP2 murine hepatocytes. Data are shown as the mean ± S.E.M. of three independent experiments.

B) (Left panel) Western blot analysis for PCBP2 on protein extracts from hepatocytes silenced for PCBP2 (3A shPCBP2) and relative control (3A shCTR). GAPDH has been used as loading control. The figure is representative of three independent experiments. (Right panel) Densitometric analysis of Western blot signals. Data are shown as the mean ± S.E.M. of three independent experiments.

Then 3A shCTR and shPCBP2 cell lines were cultured for 72 hours to allow the production of extracellular vesicles and conditioned media were collected to isolate the EVs. EVs obtained by ultracentrifugation were characterized based on the expression of typical markers (by western blot) and of their size and concentration by Tunable Resistive Pulse Sensing (TRPS) technology using Exoid (Izon Science) (figure 4A-B).

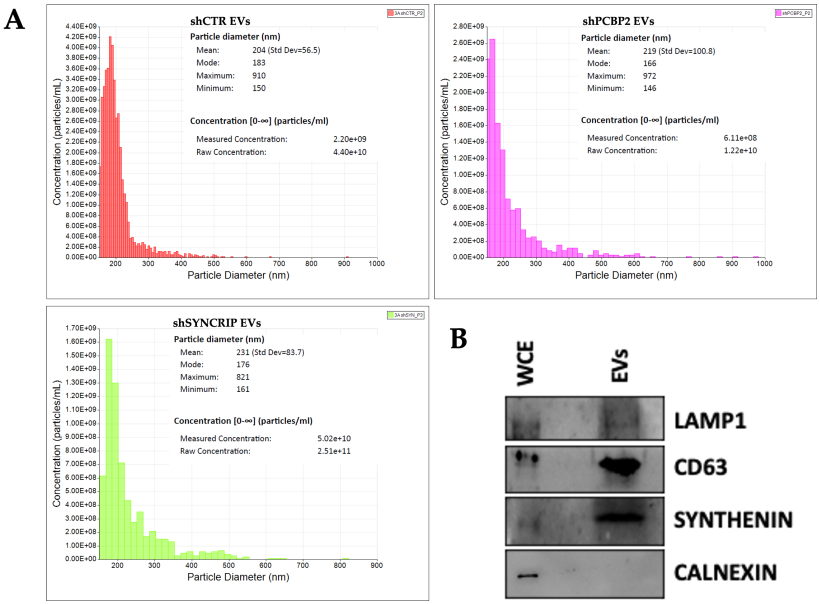

Figure 4. EVs characterization

A) Particle diameter (nm) and concentration (particles/ml) of EVs evaluated by Exoid (IZON). Histograms report the concentration (particles/ml) by size (nm) for each of the three analyzed conditions (left panel: shCTR EVs; right panel: shPCBP2 EVs; bottom panel shSYNCRIP EVs).

B) Western blot analysis for EV-specific (LAMP1-CD63-Synthenin) and intracellular (calnexin) markers on protein extracts from hepatocytes (WCE, whole cell extract) and hepatocyte-derived EVs (EVs).

Notably, PCBP2 interference enhances miRNA-155-3p loading in EVs with respect to control cell-derived EVs (figure 5, left panel). As a further control that miRNAs without the CELL motif are not affected by PCBP2 silencing, the expression levels of miR-365-2-5p

(embedding the sole hEXO motif) were analyzed in EVs and cells, and resulted not differentially exported (figure 5, middle panel).

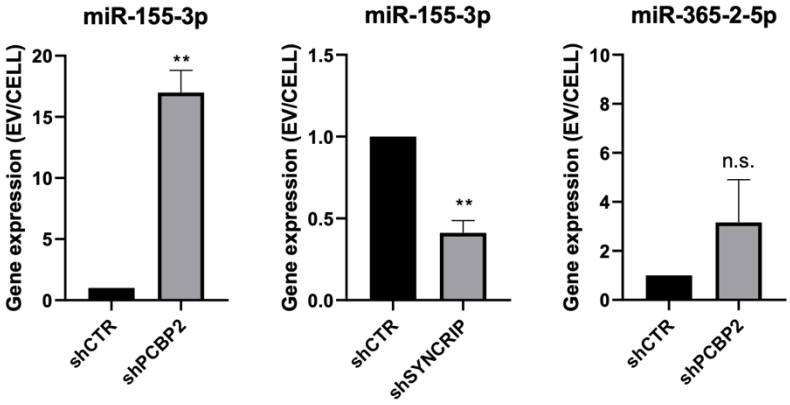

Figure 5. PCBP2 has a functional role in intracellular retention of miRNA-155-3p

(left and middle panels) EV miRNA-155-3p and miR-365-2-5p levels in shCTR and shPCBP2 cells analyzed by RT-qPCR. Data are expressed as ratio of miRNA expression in EVs with respect to the intracellular compartment (shCTR arbitrary value 1). Results are shown as the mean ± S.E.M. of three independent experiments.

(right panel) EV miRNA-155-3p levels in shCTR and shSYNCRIP cells analyzed by RT-qPCR. Data are expressed as ratio of miRNA expression in EVs with respect to the intracellular compartment (shCTR arbitrary value 1). Results are shown as the mean ± S.E.M. of three independent experiments. Data are considered statistically significant with $p < 0.05$ (Student's T test). *: $p<0.05$; **: $p<0.01$.

Since miR-155-3p bears hEXO motif and, as previously demonstrated, is bound by SYNCRIP, we also analyzed the effect of SYNCRIP silencing (obtained by an shRNA approach and validated in figure

6A-B) on the compartmentalization of this miRNA.

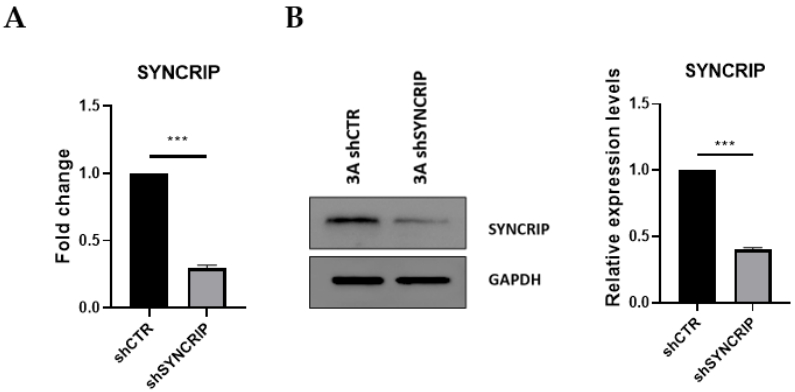

Figure 6. SYNCRIP silencing

A) Expression levels of syncrip in shCTR and shSYNCRIP murine hepatocytes. Data are shown as the mean ± S.E.M. of three independent experiments.

B) (Left panel) Western-blot analysis for SYNCRIP on protein extracts from hepatocytes silenced for SYNCRIP (3A shSYNCRIP) and relative control (3A shCTR). GAPDH has been used as loading control. The figure is representative of three independent experiments.

(Right panel) Densitometric analysis of Western-blot signals. Data are shown as the mean ± S.E.M. of three independent experiments.

As expected, SYNCRIP silencing reduces miR-155-3p export into EVs (figure 5, right panel); (for EVs characterization see figure 4).

Overall, these data demonstrated that *i)* PCBP2 interacts with miRNA-155-3p, as proved by RIP analysis and RNA pull-down, *ii)* the interaction is CELL-motif-dependent while an unexpected role for the

hEXO motif is also unveiled and *iii)* PCBP2 favors the intracellular localization of this miRNA.

2. PCBP2 binding to miR-155-3p is both sequence- and SYNCRIP-dependent

The observation that loading (hEXO) and retention (CELL) motifs are both present in miR-155-3p sequence prompted us to investigate the hypothesis of a sequence- and SYNCRIP-dependent PCBP2 binding ability.

First, co-immunoprecipitation experiments demonstrated PCBP2-SYNCRIP interaction (figure 7A) and more interestingly that both RBPs bind to miR-155-3p contemporarily as indicated by the ultra-shift obtained in electrophoretic mobility shift assay (EMSA) using both anti-PCBP2 and anti-SYNCRIP antibodies (figure 7B).

To challenge the hypothesis of a SYNCRIP-dependent PCBP2 binding, EMSA assay was performed in PCBP2-silenced and in SYNCRIP-silenced cells. As shown in figure 7C, while the PCBP2 silencing does not affect SYNCRIP binding, SYNCRIP silencing impairs also PCBP2 binding. Furthermore, RIP assay was performed on SYNCRIP-silenced cells; as shown in figure 7D, SYNCRIP silencing impairs PCBP2 binding to miR-155-3p.

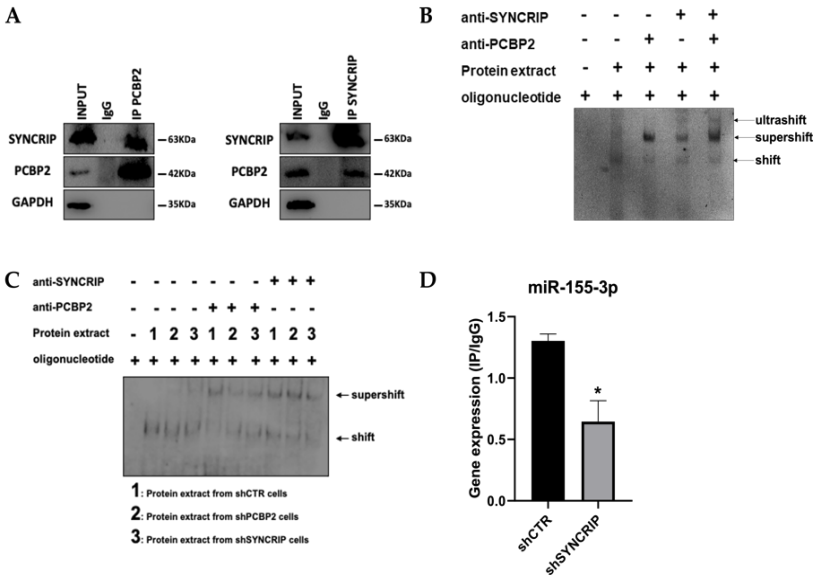

Figure 7. PCBP2 binding to miR-155-3p is both sequence- and SYNCRIP-dependent

A) Co-immunoprecipitation of PCBP2 and SYNCRIP. Immunoprecipitations with rabbit polyclonal anti-PCBP2, mouse monoclonal anti-SYNCRIP and the relative pre-immune IgG were performed on protein extracts from hepatocytes. GAPDH is used as negative control. Immunoblots representative of three independent experiments are shown.

B) Electrophoretic mobility shift assay (EMSA): interactions of miR-155-3p with the indicated protein extracts (shifts) and Abs (anti-SYNCRIP and anti-PCBP2) (supershift) are shown. Ultrashift shown in lane 5 demonstrates concurrent binding of SYNCRIP and PCBP2 to miR-155-3p.

C) Electrophoretic mobility shift assay (EMSA): interactions of miR-155-3p with protein extracts from shCTR (1), shPCBP2 (2) and shSYNCRIP (3) cells (shifts) and Abs (anti-SYNCRIP and anti-PCBP2) (supershift) are shown.

D) UV-crosslinking RIP of PCBP2 protein in murine hepatocytes both WT (shCTR) and silenced for SYNCRIP (shSYNCRIP). RT-qPCR analysis for the expression of miR-155-3p is shown as IP/IgG. Data are the mean ± SEM of three independent experiments.

This evidence supports the unpredictable mechanism where SYNCRIP binding appears a prerequisite for PCBP2 recruitment. To further confirm and extend this observation, several mutants of distinct miRNAs were designed and tested by RNA pull-down for the binding capacity of these two proteins.

Results indicate that mutagenesis of the sole hEXO motif (miR26b-3p no-hEXO) on miR-26 backbone (bearing both hEXO and CELL motifs), impairs also PCBP2 binding (figure 8A) and conversely the *de novo* inclusion of a hEXO motif in miR-31-3p backbone (bearing only CELL-motifs) (miR-31-3p +hEXO) confers a *de novo* PCBP2 binding ability to this mutant; furthermore, mutation in the CELL motif on miR-31-3p including the hEXO (miR-31-3p +hEXO no-CELL) impairs PCBP2 binding (figure 8B).

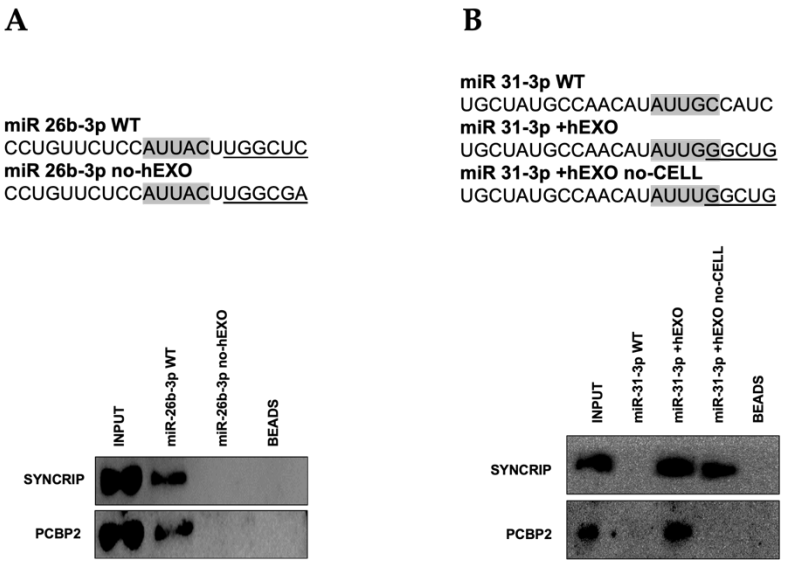

Figure 8. hEXO and CELL motifs are propaedeutic to PCBP2 binding

A) RNA pull-down with the WT and mutated (sequences are reported above) miR-26b-3p followed by western blot for the indicated proteins. Data are representative of three independent experiments.

B) RNA pull-down with the WT and mutated (sequences are reported above) miR-31-3p followed by western blot for the indicated proteins. Data are representative of three independent experiments.

Data are considered statistically significant with $p < 0.05$ (Student's T test). *: $p<0.05$.

A-B) CELL motifs (WT and mutated) are shown in grey, hEXO motifs (WT and mutated) are underlined.

Overall, these data indicate that PCBP2 binding requires both the CELL motif and SYNCRIP binding; in other words, SYNCRIP binding is epistatic to PCBP2 recruitment.

3. PCBP2 functionally dominates on SYNCRIP EV-loading activity on a repertoire of miRNAs embedding CELL and hEXO motifs

To extend the evidence on the role of PCBP2 in miRNA compartmentalization and to confirm the disclosed mechanism, PCBP2 and SYNCRIP functional role in miRNA EVs/cell partition was evaluated. First, we performed an NGS analysis of miRNAs exported in EVs produced by control and PCBP2-silenced murine hepatocytes; this wide range observation allowed the selection of further miRNAs differentially loaded in EVs in correlation to PCBP2 expression. Then, PCBP2 functional role was assessed by means of qRT-PCR performed on 9 miRNAs expressed in EVs and embedding both CELL and hEXO motifs in extra-seed position, as identified by bioinformatic motif scanning analysis, in comparison to 2 miRNAs embedding either the CELL or the hEXO motif (figure 9A).

In order to consider a possible impact of PCBP2 on miRNAs' steady state level (resulting from variation in transcription and biogenesis), miRNA abundance in EVs and in the intracellular compartment was analyzed by qRT-PCR as EVs/cell ratio. Results indicate that PCBP2 silencing enhances miRNAs loading into EVs (figure 9B); thus, highlighting a dominant PCBP2 cell-retention function on the confirmed SYNCRIP-dependent export (figure 9C).

A

miRNA	Sequence
mmu-miR-345-3p	CCCUGAACUAGGGGUCUGGAGAC
mmu-miR-23a-5p	GGGGUUCCUGGGGAUGGGAUUU
mmu-miR-214-3p	ACAGCAGGCACAGACAGGCAGU
mmu-miR-155-5p	UUAAUGCUAAUUGUGAUAGGGGU
mmu-miR-181d-5p	AACAUUCAUUGUUGUCGGUGGGU
mmu-miR-3084-5p	GUUGAAGGUUAAUUAGCAGAGU
mmu-miR-122b-3p	AAACACCAUUGUCACACUCCAC
mmu-miR-192-5p	CUGACCUAUGAAUUGACAGCC
mmu-miR-26b-3p	CCUGUUCUCCAUUACUUGGCUC
mmu-miR 365-2-5p	AGGGACUUUCAGGGGCAGCUGUG
mmu-miR 31-3p	UGCUAUGCCAACAUAUUGCCAUC

CELL: CELL motif hEXO: hEXO motif

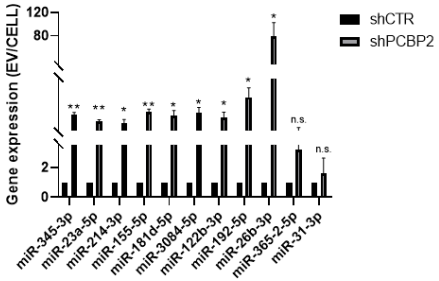

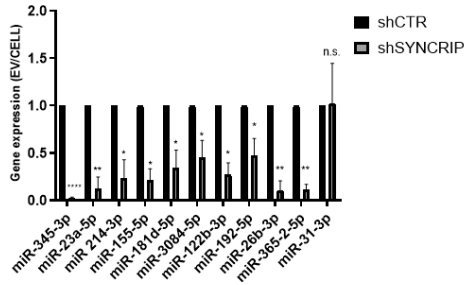

Figure 9. PCBP2 functionally dominates on SYNCRIP EV-loading activity on a repertoire of miRNAs embedding CELL and hEXO motifs

A) List of selected miRNAs embedding CELL and/or hEXO motifs; consensus sequences are highlighted in grey or underlined respectively.

B) EV miRNA levels in shCTR and shPCBP2 cells analyzed by RT-qPCR. Data are expressed as ratio of miRNA expression in EVs with respect to the intracellular compartment (shCTR arbitrary value 1). Results are shown as the mean ± S.E.M. of three independent experiments.

Data are considered statistically significant with p< 0.05 (Student's T test). *: p<0.05; **: p<0.01.
C) EV miRNA levels in shCTR and shSYNCRIP cells analyzed by RT-qPCR. Data are expressed as ratio of miRNA expression in EVs with respect to the intracellular compartment (shCTR arbitrary value 1). Results are shown as the mean ± S.E.M. of three independent experiments.
Data are considered statistically significant with p< 0.05 (Student's T test). *: p<0.05; **: p<0.01; ****: p<0.0001.

In order to understand the molecular mechanism, we performed RIP-qPCR assay and we demonstrated that PCBP2 is able to bind miRNAs embedding the CELL and hEXO motifs (miRs-345-3p, 23a-5p, 214-3p, 155-5p, 181d-5p, 3084-5p, 122b-3p, 192-5p, 26b-3p); conversely, the presence of either the sole hEXO in miR-365-2-5p or the sole CELL in miR-31-3p does not allow PCBP2 binding (figure 10A). As expected, the presence of the hEXO motif alone or in combination with the CELL motif is sufficient for SYNCRIP binding to all the analyzed miRNAs (figure 10B).

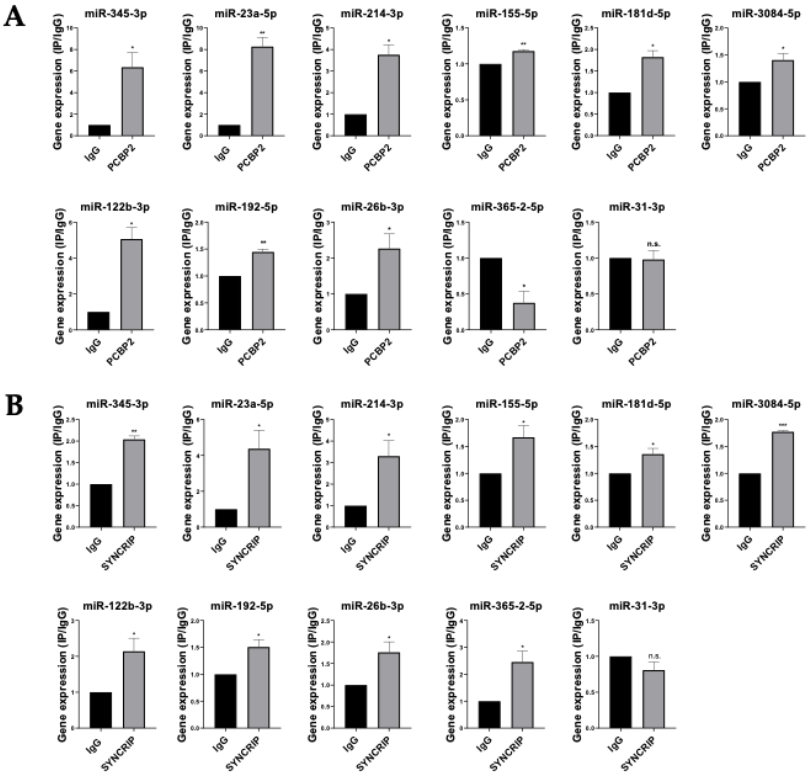

Figure 10. PCBP2 and SYNCRIP display a different binding capacity

A) UV-crosslinking RIP of PCBP2 protein in murine hepatocytes. RT-qPCR analysis for the indicated miRNAs is shown as IP/IgG for each independent experiment (IgG arbitrary value 1). Data are the mean ± SEM of three independent experiments.

Data are considered statistically significant with $p < 0.05$ (Student's T test). *: $p<0.05$; **: $p<0.01$.

B) UV-crosslinking RIP of SYNCRIP protein in murine hepatocytes. RT-qPCR analysis for the indicated miRNAs is shown as IP/IgG for each independent experiment (IgG arbitrary value 1). Data are the mean ± SEM of three independent experiments.

Furthermore, in line with data obtained for miR-155-3p, results shown in figure 11 demonstrate the SYNCRIP-dependent PCBP2 binding assessed in hepatocytes silenced for SYNCRIP.

Overall, these data indicate that the previously described SYNCRIP capacity to act as EV loader is functionally limited by the presence of a here-identified sequence- and SYNCRIP-dependent retention mechanism mediated by the RNA-binding protein PCBP2.

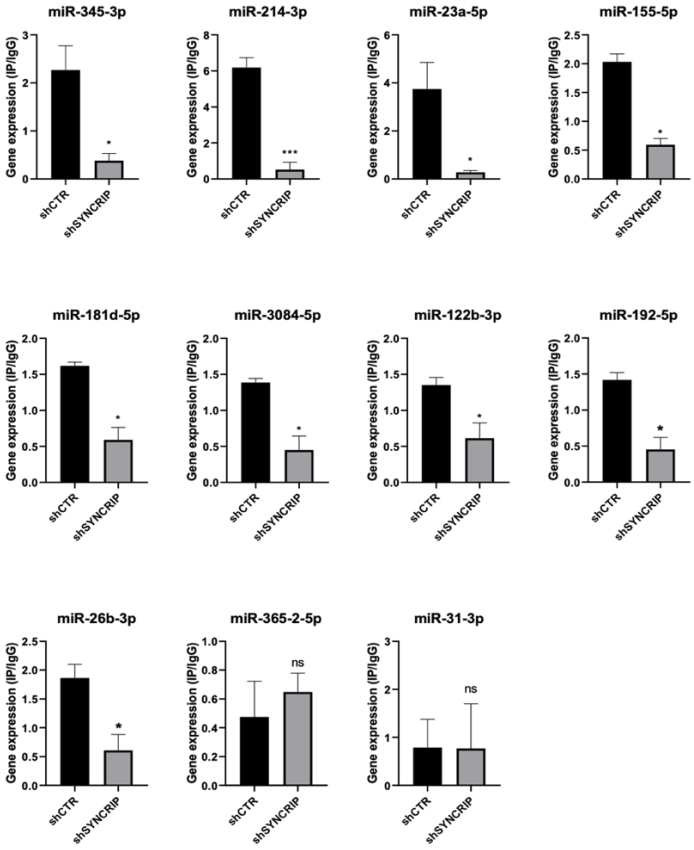

Figure 11. PCBP2 binding to miRNA embedding CELL and hEXO motif is SYNCRIP-dependent

UV-crosslinking RIP of PCBP2 protein in murine hepatocytes both WT (shCTR) and silenced for SYNCRIP (shSYNCRIP). RT-qPCR analysis for the indicated miRNAs is shown as IP/IgG. Data are the mean ± SEM of three independent experiments. Data are considered statistically significant with $p< 0.05$ (Student's T test). *: $p<0.05$; ***: $p<0.001$.

DISCUSSION

The processes controlling the selective partition of miRNAs between intracellular and EV compartments, in both physiology and disease, are still largely uncharacterized. However, it is known that the presence of short consensus sequences mediates miRNAs sorting: indeed, the CELL and the EXO motifs are responsible for intracellular retention or EVs sorting respectively[93,98].

With respect to miRNA EV-loading, it has also been reported that these sequence-dependent mechanisms of export are mediated by several RBPs. In particular, the proteins hnRNPA2B1, ALYREF and FUS have been identified and characterized at the molecular and functional levels as interactors and carriers of EXO-motif-embedding miRNAs into EVs.

Moreover, our research group dissected the functional and structural role of the hnRNP SYNCRIP as a component of the hepatocytes-derived EVs miRNA sorting machinery, allowing the EVs loading of a specific set of miRNAs that share the hEXO motif in their sequence[96].

While the molecular players responsible for miRNA loading into EVs have been partially unveiled, the mechanism involved in miRNA intracellular retention remains largely uncharacterized. Even if the

role of the CELL motifs has been demonstrated by means of functional assays involving the introduction/removal of these sequences into different miRNAs, no data are currently available on the RBPs involved in the recognition of these consensus motifs and thus in miRNA cell retention. This gap of knowledge prompted us to investigate the molecular players responsible for miRNAs intracellular retention.

The main finding of this investigation is the identification of PCBP2 as a new regulator of miRNA partition between intracellular and EV compartments.

PCBP2 protein is an RNA-binding protein with pleiotropic functions; specifically, it is a well-characterized member of the Poly-rC-binding proteins (PCBPs), a group of multifunctional RNA-binding proteins that contain three highly conserved RNA binding KH domains and that may shuttle between the nucleus and the cytoplasm[130]. A large body of evidence points to its role in controlling multiple processes including RNA maturation and trafficking, RNA editing, translational activation or repression and mRNA degradation[104,106,157-160].

The here provided results demonstrated that PCBP2 binds to the miRNA 155-3p, containing one of the CELL-motif previously identified by *in silico* sequence analysis on miRNAs retained in the cytoplasm of AML12 mouse hepatocytes[98] (figure 2A). Moreover, based on small RNA sequencing performed by Santangelo and

colleagues, this miRNA is among the top 20 cell-retained miRNAs in hepatocytes[96].

PCBP2 interaction with this miRNA is dependent on the CELL motif, located in extra-seed position; indeed, the introduction of a CELL motif-specific permutation impairs PCBP2 binding to miR-155-3p (figures 1A-B and 2B).

Further evidence for the requirement of PCBP2 and CELL motif interaction is the absence of interaction between PCBP2 and miRNA 365-2-5p, devoid of CELL motif, and enriched in hepatocytes-derived EVs, based on data from[96] (figure 2C).

Interestingly, the inspection of the miR-155-3p sequence revealed the presence of the previously identified SYNCRIP binding site, the hEXO motif: biochemical assays demonstrated SYNCRIP binding to miRNA-155-3p and confirmed that this interaction is hEXO motif-dependent, in line with proteomic analysis (figures 1A-B, 2B-E).

SYNCRIP is a pleiotropic regulator of gene expression at the post-transcriptional and translational level from pre-mRNA splicing, RNA editing and cytoplasmic mRNA transport to internal ribosome entry site (IRES)-mediated translational activation and mRNA degradation[112-114]. SYNCRIP is also involved in differentiation and in the progression of different types of cancers including leukemia, breast cancer, colorectal cancer and liver cancer[117,161,162].

Based on the biochemical evidence obtained by RIP and RNA pull-down with wild type and mutated oligonucleotides, the potential synergic or mutually exclusive binding of PCBP2 to SYNCRIP-bound miRNA was also evaluated. Surprisingly, PCBP2 binding to miRNA 155-3p is not simply dependent on its specific CELL motif but also requires SYNCRIP; indeed, hEXO motif mutation or SYNCRIP silencing impair PCBP2 binding to this miRNA (figures 2B and 7C-D). So, we describe an unpredictable mechanism where PCBP2 binding is dependent on SYNCRIP recruitment to miRNA 155-3p.

Moreover, the observation that PCBP2 and SYNCRIP bind to miRNA 155-3p at the same time, in addition to exclude that PCBP2 and SYNCRIP binding is mutually exclusive, supports our observed mechanism (figure 7B).

Furthermore, the absence of interaction between PCBP2 and miRNA 31-3p, devoid of the hEXO motif, and unable to interact with PCBP2, provide a further proof of the validity of the proposed model (figure 2A).

This mechanism was also verified on miRNA 26b-3p and 31-3p by using specific insertion/removal mutants: PCBP2 doesn't bind to miRNA 26b-3p upon the mutation of the hEXO motif despite the CELL motif conservation; conversely, in miRNA 31-3p, PCBP2 acquires binding capacity to CELL motif in response to the hEXO introduction (figure 8).

The proposed mechanism of SYNCRIP, PCBP2 and SYNCRIP-dependent PCBP2 binding to miRNA 155-3p was also extended by RIP analysis on further 9 miRNAs selected on the basis of an NGS approach and of a bioinformatic analysis (figure 9A). Overall, our data evidence that PCBP2 and SYNCRIP display different binding capacity to miRNAs: PCBP2 binds to miRNAs embedding CELL motif but also requires hEXO motif; conversely SYNCRIP binds miRNAs embedding hEXO motif, regardless the presence of the CELL motif (figure 10).

Notably, the obtained results strongly suggested that the identified mechanism has a general relevance, being confirmed on a significant set of miRNAs (figure 11).

Of note, among them, miRs-155-3p, 23a-5p, 155-5p,192-5p and 26b-3p display important EV-mediated functions in relation to pathophysiology[163-166].

For this reason, the role of PCBP2 in miRNA partition between intracellular compartment and EVs was evaluated. Functionally our results disclosed that PCBP2 promotes cellular retention of SYNCRIP-bound miRNAs (figures 5-9B).

The added value of this work, with respect to the state of the art on this topic is that while SYNCRIP EV-loading activity has been previously well characterized by means of both functional and

structural analysis, the role of PCBP2 as mediator of miRNA intracellular retention is here disclosed for the first time.

The here proposed mechanism implies that the export activity of SYNCRIP is specifically impaired by PCBP2 and highlights that the miRNA partition is not only related to the presence of specific RBPs/export sequences interaction but depends on the equilibrium and on the functional interaction among different RBPs recognizing different sequence motifs.

By summarizing, the final functional compartmentalization output appears the result of an integrated system of RNA/proteins interactions, here only partially unveiled, whose dynamics may provide elements for the explanation of the EVs miRNA cargo specificity and for its variation coherently to cellular plasticity. Worth of note, recent research highlights a further level of complexity since miRNA epitranscriptomic modifications, while impairing miRNA intracellular function, appear instrumental to miRNA loading in EVs[99]. This concept, now limited to the RBP A2B1, should be extended to other RBPs exerting different roles in these intricate dynamics.

Altogether, evidence here gathered indicates that: i) PCBP2 binding requires both the miRNA CELL sequence and the RBP SYNCRIP, which in turn recognizes its specific hEXO consensus; in other words, SYNCRIP binding is a prerequisite for PCBP2 recruitment; ii) PCBP2 cell retention function is dominant over the EV-loading SYNCRIP one;

in other words, PCBP2 impairs SYNCRIP-mediated miRNA export (figure 12).

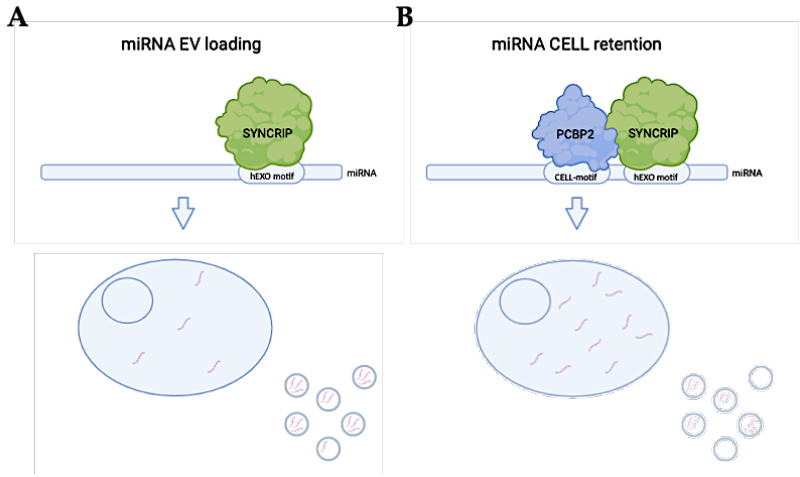

Figure 12. Schematic model of PCBP2/SYNCRIP dependent miRNAs compartmentalization.
A) hEXO-SYNCRIP interaction promotes miRNAs secretion into EVs.
B) SYNCRIP-dependent PCBP2-CELL motif interaction promotes miRNAs intracellular retention.

The described multiple RNA/proteins interactions provide a further step in the process of clarification of the mechanisms that control cellular communication in pathophysiological processes. The knowledge of molecular players of miRNAs intracellular/EVs partition could be soon instrumental for the development of RNA-based manipulations holding therapeutic perspectives with the intent to design and apply novel strategies for a personalized medicine.

REFERENCES

1. Deatherage, B.L., and Cookson, B.T. (2012). Membrane vesicle release in bacteria, eukaryotes, and archaea: a conserved yet underappreciated aspect of microbial life. Infect Immun *80*, 1948-1957. 10.1128/IAI.06014-11.
2. Robinson, D.G., Ding, Y., and Jiang, L. (2016). Unconventional protein secretion in plants: a critical assessment. Protoplasma *253*, 31-43. 10.1007/s00709-015-0887-1.
3. Schorey, J.S., Cheng, Y., Singh, P.P., and Smith, V.L. (2015). Exosomes and other extracellular vesicles in host-pathogen interactions. EMBO Rep *16*, 24-43. 10.15252/embr.201439363.
4. Lasser, C., Jang, S.C., and Lotvall, J. (2018). Subpopulations of extracellular vesicles and their therapeutic potential. Mol Aspects Med *60*, 1-14. 10.1016/j.mam.2018.02.002.
5. van Niel, G., Carter, D.R.F., Clayton, A., Lambert, D.W., Raposo, G., and Vader, P. (2022). Challenges and directions in studying cell-cell communication by extracellular vesicles. Nat Rev Mol Cell Biol *23*, 369-382. 10.1038/s41580-022-00460-3.
6. Tricarico, C., Clancy, J., and D'Souza-Schorey, C. (2017). Biology and biogenesis of shed microvesicles. Small GTPases *8*, 220-232. 10.1080/21541248.2016.1215283.
7. Gurung, S., Perocheau, D., Touramanidou, L., and Baruteau, J. (2021). The exosome journey: from biogenesis to uptake and intracellular signalling. Cell Commun Signal *19*, 47. 10.1186/s12964-021-00730-1.
8. Dixson, A.C., Dawson, T.R., Di Vizio, D., and Weaver, A.M. (2023). Context-specific regulation of extracellular vesicle

biogenesis and cargo selection. Nat Rev Mol Cell Biol *24*, 454-476. 10.1038/s41580-023-00576-0.

9. Thery, C., Witwer, K.W., Aikawa, E., Alcaraz, M.J., Anderson, J.D., Andriantsitohaina, R., Antoniou, A., Arab, T., Archer, F., Atkin-Smith, G.K., et al. (2018). Minimal information for studies of extracellular vesicles 2018 (MISEV2018): a position statement of the International Society for Extracellular Vesicles and update of the MISEV2014 guidelines. J Extracell Vesicles *7*, 1535750. 10.1080/20013078.2018.1535750.
10. Kowal, J., Arras, G., Colombo, M., Jouve, M., Morath, J.P., Primdal-Bengtson, B., Dingli, F., Loew, D., Tkach, M., and Thery, C. (2016). Proteomic comparison defines novel markers to characterize heterogeneous populations of extracellular vesicle subtypes. Proc Natl Acad Sci U S A *113*, E968-977. 10.1073/pnas.1521230113.
11. van Niel, G., D'Angelo, G., and Raposo, G. (2018). Shedding light on the cell biology of extracellular vesicles. Nat Rev Mol Cell Biol *19*, 213-228. 10.1038/nrm.2017.125.
12. Jeppesen, D.K., Fenix, A.M., Franklin, J.L., Higginbotham, J.N., Zhang, Q., Zimmerman, L.J., Liebler, D.C., Ping, J., Liu, Q., Evans, R., et al. (2019). Reassessment of Exosome Composition. Cell *177*, 428-445 e418. 10.1016/j.cell.2019.02.029.
13. Gusachenko, O.N., Zenkova, M.A., and Vlassov, V.V. (2013). Nucleic acids in exosomes: disease markers and intercellular communication molecules. Biochemistry (Mosc) *78*, 1-7. 10.1134/S000629791301001X.
14. Marima, R., Basera, A., Miya, T., Damane, B.P., Kandhavelu, J., Mirza, S., Penny, C., and Dlamini, Z. (2024). Exosomal long non-coding RNAs in cancer: Interplay, modulation, and therapeutic avenues. Noncoding RNA Res *9*, 887-900. 10.1016/j.ncrna.2024.03.014.
15. Wu, S., Yang, T., Ma, M., Fan, L., Ren, L., Liu, G., Wang, Y., Cheng, B., Xia, J., and Hao, Z. (2024). Extracellular vesicles

meet mitochondria: Potential roles in regenerative medicine. Pharmacol Res *206*, 107307. 10.1016/j.phrs.2024.107307.

16. Balaj, L., Lessard, R., Dai, L., Cho, Y.J., Pomeroy, S.L., Breakefield, X.O., and Skog, J. (2011). Tumour microvesicles contain retrotransposon elements and amplified oncogene sequences. Nat Commun *2*, 180. 10.1038/ncomms1180.
17. Kahlert, C., Melo, S.A., Protopopov, A., Tang, J., Seth, S., Koch, M., Zhang, J., Weitz, J., Chin, L., Futreal, A., and Kalluri, R. (2014). Identification of double-stranded genomic DNA spanning all chromosomes with mutated KRAS and p53 DNA in the serum exosomes of patients with pancreatic cancer. J Biol Chem *289*, 3869-3875. 10.1074/jbc.C113.532267.
18. Lee, Y.J., Shin, K.J., and Chae, Y.C. (2024). Regulation of cargo selection in exosome biogenesis and its biomedical applications in cancer. Exp Mol Med *56*, 877-889. 10.1038/s12276-024-01209-y.
19. Juan, T., and Fürthauer, M. (2018). Biogenesis and function of ESCRT-dependent extracellular vesicles. Semin Cell Dev Biol *74*, 66-77. 10.1016/j.semcdb.2017.08.022.
20. Raiborg, C., and Stenmark, H. (2009). The ESCRT machinery in endosomal sorting of ubiquitylated membrane proteins. Nature *458*, 445-452. 10.1038/nature07961.
21. Babst, M., Katzmann, D.J., Snyder, W.B., Wendland, B., and Emr, S.D. (2002). Endosome-associated complex, ESCRT-II, recruits transport machinery for protein sorting at the multivesicular body. Dev Cell *3*, 283-289. 10.1016/s1534-5807(02)00219-8.
22. Babst, M., Katzmann, D.J., Estepa-Sabal, E.J., Meerloo, T., and Emr, S.D. (2002). Escrt-III: an endosome-associated heterooligomeric protein complex required for mvb sorting. Dev Cell *3*, 271-282. 10.1016/s1534-5807(02)00220-4.
23. Coonrod, E.M., and Stevens, T.H. (2010). The yeast vps class E mutants: the beginning of the molecular genetic analysis of

multivesicular body biogenesis. Mol Biol Cell *21*, 4057-4060. 10.1091/mbc.E09-07-0603.

24. Trajkovic, K., Hsu, C., Chiantia, S., Rajendran, L., Wenzel, D., Wieland, F., Schwille, P., Brügger, B., and Simons, M. (2008). Ceramide triggers budding of exosome vesicles into multivesicular endosomes. Science *319*, 1244-1247. 10.1126/science.1153124.
25. Goñi, F.M., and Alonso, A. (2009). Effects of ceramide and other simple sphingolipids on membrane lateral structure. Biochim Biophys Acta *1788*, 169-177. 10.1016/j.bbamem.2008.09.002.
26. Wei, D., Zhan, W., Gao, Y., Huang, L., Gong, R., Wang, W., Zhang, R., Wu, Y., Gao, S., and Kang, T. (2021). RAB31 marks and controls an ESCRT-independent exosome pathway. Cell Res *31*, 157-177. 10.1038/s41422-020-00409-1.
27. Perez-Hernandez, D., Gutiérrez-Vázquez, C., Jorge, I., López-Martín, S., Ursa, A., Sánchez-Madrid, F., Vázquez, J., and Yáñez-Mó, M. (2013). The intracellular interactome of tetraspanin-enriched microdomains reveals their function as sorting machineries toward exosomes. J Biol Chem *288*, 11649-11661. 10.1074/jbc.M112.445304.
28. Chairoungdua, A., Smith, D.L., Pochard, P., Hull, M., and Caplan, M.J. (2010). Exosome release of β-catenin: a novel mechanism that antagonizes Wnt signaling. J Cell Biol *190*, 1079-1091. 10.1083/jcb.201002049.
29. Zimmerman, B., Kelly, B., McMillan, B.J., Seegar, T.C.M., Dror, R.O., Kruse, A.C., and Blacklow, S.C. (2016). Crystal Structure of a Full-Length Human Tetraspanin Reveals a Cholesterol-Binding Pocket. Cell *167*, 1041-1051.e1011. 10.1016/j.cell.2016.09.056.
30. Géminard, C., De Gassart, A., Blanc, L., and Vidal, M. (2004). Degradation of AP2 during reticulocyte maturation enhances binding of hsc70 and Alix to a common site on TFR for sorting

into exosomes. Traffic *5*, 181-193. 10.1111/j.1600-0854.2004.0167.x.

31. Baietti, M.F., Zhang, Z., Mortier, E., Melchior, A., Degeest, G., Geeraerts, A., Ivarsson, Y., Depoortere, F., Coomans, C., Vermeiren, E., et al. (2012). Syndecan-syntenin-ALIX regulates the biogenesis of exosomes. Nat Cell Biol *14*, 677-685. 10.1038/ncb2502.
32. Imjeti, N.S., Menck, K., Egea-Jimenez, A.L., Lecointre, C., Lembo, F., Bouguenina, H., Badache, A., Ghossoub, R., David, G., Roche, S., and Zimmermann, P. (2017). Syntenin mediates SRC function in exosomal cell-to-cell communication. Proc Natl Acad Sci U S A *114*, 12495-12500. 10.1073/pnas.1713433114.
33. Piper, R.C., and Katzmann, D.J. (2007). Biogenesis and function of multivesicular bodies. Annu Rev Cell Dev Biol *23*, 519-547. 10.1146/annurev.cellbio.23.090506.123319.
34. Eitan, E., Suire, C., Zhang, S., and Mattson, M.P. (2016). Impact of lysosome status on extracellular vesicle content and release. Ageing Res Rev *32*, 65-74. 10.1016/j.arr.2016.05.001.
35. Villarroya-Beltri, C., Baixauli, F., Mittelbrunn, M., Fernández-Delgado, I., Torralba, D., Moreno-Gonzalo, O., Baldanta, S., Enrich, C., Guerra, S., and Sánchez-Madrid, F. (2016). ISGylation controls exosome secretion by promoting lysosomal degradation of MVB proteins. Nat Commun *7*, 13588. 10.1038/ncomms13588.
36. Hessvik, N.P., and Llorente, A. (2018). Current knowledge on exosome biogenesis and release. Cell Mol Life Sci *75*, 193-208. 10.1007/s00018-017-2595-9.
37. Ostrowski, M., Carmo, N.B., Krumeich, S., Fanget, I., Raposo, G., Savina, A., Moita, C.F., Schauer, K., Hume, A.N., Freitas, R.P., et al. (2010). Rab27a and Rab27b control different steps of the exosome secretion pathway. Nat Cell Biol *12*, 19-30; sup pp 11-13. 10.1038/ncb2000.

38. Jahn, R., and Scheller, R.H. (2006). SNAREs--engines for membrane fusion. Nat Rev Mol Cell Biol *7*, 631-643. 10.1038/nrm2002.
39. Liu, C., Liu, D., Wang, S., Gan, L., Yang, X., and Ma, C. (2023). Identification of the SNARE complex that mediates the fusion of multivesicular bodies with the plasma membrane in exosome secretion. J Extracell Vesicles *12*, e12356. 10.1002/jev2.12356.
40. Gross, J.C., Chaudhary, V., Bartscherer, K., and Boutros, M. (2012). Active Wnt proteins are secreted on exosomes. Nat Cell Biol *14*, 1036-1045. 10.1038/ncb2574.
41. Hyenne, V., Apaydin, A., Rodriguez, D., Spiegelhalter, C., Hoff-Yoessle, S., Diem, M., Tak, S., Lefebvre, O., Schwab, Y., Goetz, J.G., and Labouesse, M. (2015). RAL-1 controls multivesicular body biogenesis and exosome secretion. J Cell Biol *211*, 27-37. 10.1083/jcb.201504136.
42. Koles, K., and Budnik, V. (2012). Exosomes go with the Wnt. Cell Logist *2*, 169-173. 10.4161/cl.21981.
43. Sobo-Vujanovic, A., Munich, S., and Vujanovic, N.L. (2014). Dendritic-cell exosomes cross-present Toll-like receptor-ligands and activate bystander dendritic cells. Cell Immunol *289*, 119-127. 10.1016/j.cellimm.2014.03.016.
44. Tkach, M., Kowal, J., Zucchetti, A.E., Enserink, L., Jouve, M., Lankar, D., Saitakis, M., Martin-Jaular, L., and Théry, C. (2017). Qualitative differences in T-cell activation by dendritic cell-derived extracellular vesicle subtypes. EMBO J *36*, 3012-3028. 10.15252/embj.201696003.
45. Prada, I., and Meldolesi, J. (2016). Binding and Fusion of Extracellular Vesicles to the Plasma Membrane of Their Cell Targets. Int J Mol Sci *17*. 10.3390/ijms17081296.
46. Abels, E.R., and Breakefield, X.O. (2016). Introduction to Extracellular Vesicles: Biogenesis, RNA Cargo Selection, Content, Release, and Uptake. Cell Mol Neurobiol *36*, 301-312. 10.1007/s10571-016-0366-z.

47. Mettlen, M., Chen, P.H., Srinivasan, S., Danuser, G., and Schmid, S.L. (2018). Regulation of Clathrin-Mediated Endocytosis. Annu Rev Biochem *87*, 871-896. 10.1146/annurev-biochem-062917-012644.
48. Kiss, A.L., and Botos, E. (2009). Endocytosis via caveolae: alternative pathway with distinct cellular compartments to avoid lysosomal degradation? J Cell Mol Med *13*, 1228-1237. 10.1111/j.1582-4934.2009.00754.x.
49. Xu, Y.P., Jiang, T., Yang, X.F., and Chen, Z.B. (2024). Methods, Mechanisms, and Application Prospects for Enhancing Extracellular Vesicle Uptake. Curr Med Sci *44*, 247-260. 10.1007/s11596-024-2861-7.
50. Nabi, I.R., and Le, P.U. (2003). Caveolae/raft-dependent endocytosis. J Cell Biol *161*, 673-677. 10.1083/jcb.200302028.
51. Feng, D., Zhao, W.L., Ye, Y.Y., Bai, X.C., Liu, R.Q., Chang, L.F., Zhou, Q., and Sui, S.F. (2010). Cellular internalization of exosomes occurs through phagocytosis. Traffic *11*, 675-687. 10.1111/j.1600-0854.2010.01041.x.
52. Heusermann, W., Hean, J., Trojer, D., Steib, E., von Bueren, S., Graff-Meyer, A., Genoud, C., Martin, K., Pizzato, N., Voshol, J., et al. (2016). Exosomes surf on filopodia to enter cells at endocytic hot spots, traffic within endosomes, and are targeted to the ER. J Cell Biol *213*, 173-184. 10.1083/jcb.201506084.
53. Joshi, B.S., de Beer, M.A., Giepmans, B.N.G., and Zuhorn, I.S. (2020). Endocytosis of Extracellular Vesicles and Release of Their Cargo from Endosomes. ACS Nano *14*, 4444-4455. 10.1021/acsnano.9b10033.
54. Yates, A.G., Pink, R.C., Erdbrügger, U., Siljander, P.R., Dellar, E.R., Pantazi, P., Akbar, N., Cooke, W.R., Vatish, M., Dias-Neto, E., et al. (2022). In sickness and in health: The functional role of extracellular vesicles in physiology and pathology in vivo: Part I: Health and Normal Physiology: Part I: Health and

Normal Physiology. J Extracell Vesicles *11*, e12151. 10.1002/jev2.12151.

55. Buzas, E.I. (2023). The roles of extracellular vesicles in the immune system. Nat Rev Immunol *23*, 236-250. 10.1038/s41577-022-00763-8.
56. Aloi, N., Drago, G., Ruggieri, S., Cibella, F., Colombo, P., and Longo, V. (2024). Extracellular Vesicles and Immunity: At the Crossroads of Cell Communication. Int J Mol Sci *25*. 10.3390/ijms25021205.
57. Del Conde, I., Shrimpton, C.N., Thiagarajan, P., and López, J.A. (2005). Tissue-factor-bearing microvesicles arise from lipid rafts and fuse with activated platelets to initiate coagulation. Blood *106*, 1604-1611. 10.1182/blood-2004-03-1095.
58. Chivet, M., Hemming, F., Pernet-Gallay, K., Fraboulet, S., and Sadoul, R. (2012). Emerging role of neuronal exosomes in the central nervous system. Front Physiol *3*, 145. 10.3389/fphys.2012.00145.
59. Taverna, S., Pucci, M., and Alessandro, R. (2017). Extracellular vesicles: small bricks for tissue repair/regeneration. Ann Transl Med *5*, 83. 10.21037/atm.2017.01.53.
60. Yates, A.G., Pink, R.C., Erdbrügger, U., Siljander, P.R., Dellar, E.R., Pantazi, P., Akbar, N., Cooke, W.R., Vatish, M., Dias-Neto, E., et al. (2022). In sickness and in health: The functional role of extracellular vesicles in physiology and pathology in vivo: Part II: Pathology: Part II: Pathology. J Extracell Vesicles *11*, e12190. 10.1002/jev2.12190.
61. Conigliaro, A., and Cicchini, C. (2018). Exosome-Mediated Signaling in Epithelial to Mesenchymal Transition and Tumor Progression. J Clin Med *8*. 10.3390/jcm8010026.
62. Pucci, M., Moschetti, M., Urzì, O., Loria, M., Conigliaro, A., Di Bella, M.A., Crescitelli, R., Olofsson Bagge, R., Gallo, A., Santos, M.F., et al. (2023). Colorectal cancer-derived small extracellular vesicles induce TGFβ1-mediated epithelial to

mesenchymal transition of hepatocytes. Cancer Cell Int *23*, 77. 10.1186/s12935-023-02916-8.

63. Santangelo, L., Bordoni, V., Montaldo, C., Cimini, E., Zingoni, A., Battistelli, C., D'Offizi, G., Capobianchi, M.R., Santoni, A., Tripodi, M., and Agrati, C. (2018). Hepatitis C virus direct-acting antivirals therapy impacts on extracellular vesicles microRNAs content and on their immunomodulating properties. Liver Int *38*, 1741-1750. 10.1111/liv.13700.
64. Montaldo, C., Terri, M., Riccioni, V., Battistelli, C., Bordoni, V., D'Offizi, G., Prado, M.G., Trionfetti, F., Vescovo, T., Tartaglia, E., et al. (2021). Fibrogenic signals persist in DAA-treated HCV patients after sustained virological response. J Hepatol *75*, 1301-1311. 10.1016/j.jhep.2021.07.003.
65. Goldie, B.J., Dun, M.D., Lin, M., Smith, N.D., Verrills, N.M., Dayas, C.V., and Cairns, M.J. (2014). Activity-associated miRNA are packaged in Map1b-enriched exosomes released from depolarized neurons. Nucleic Acids Res *42*, 9195-9208. 10.1093/nar/gku594.
66. Fabbiano, F., Corsi, J., Gurrieri, E., Trevisan, C., Notarangelo, M., and D'Agostino, V.G. (2020). RNA packaging into extracellular vesicles: An orchestra of RNA-binding proteins? J Extracell Vesicles *10*, e12043. 10.1002/jev2.12043.
67. Sork, H., Corso, G., Krjutskov, K., Johansson, H.J., Nordin, J.Z., Wiklander, O.P.B., Lee, Y.X.F., Westholm, J.O., Lehtiö, J., Wood, M.J.A., et al. (2018). Heterogeneity and interplay of the extracellular vesicle small RNA transcriptome and proteome. Sci Rep *8*, 10813. 10.1038/s41598-018-28485-9.
68. Brinkman, K., Meyer, L., Bickel, A., Enderle, D., Berking, C., Skog, J., and Noerholm, M. (2020). Extracellular vesicles from plasma have higher tumour RNA fraction than platelets. J Extracell Vesicles *9*, 1741176. 10.1080/20013078.2020.1741176.
69. Mittelbrunn, M., Gutiérrez-Vázquez, C., Villarroya-Beltri, C., González, S., Sánchez-Cabo, F., González, M., Bernad, A., and Sánchez-Madrid, F. (2011). Unidirectional transfer of

microRNA-loaded exosomes from T cells to antigen-presenting cells. Nat Commun *2*, 282. 10.1038/ncomms1285.

70. Baglio, S.R., Rooijers, K., Koppers-Lalic, D., Verweij, F.J., Pérez Lanzón, M., Zini, N., Naaijkens, B., Perut, F., Niessen, H.W., Baldini, N., and Pegtel, D.M. (2015). Human bone marrow- and adipose-mesenchymal stem cells secrete exosomes enriched in distinctive miRNA and tRNA species. Stem Cell Res Ther *6*, 127. 10.1186/s13287-015-0116-z.

71. Zhu, J., Lu, K., Zhang, N., Zhao, Y., Ma, Q., Shen, J., Lin, Y., Xiang, P., Tang, Y., Hu, X., et al. (2018). Myocardial reparative functions of exosomes from mesenchymal stem cells are enhanced by hypoxia treatment of the cells via transferring microRNA-210 in an nSMase2-dependent way. Artif Cells Nanomed Biotechnol *46*, 1659-1670. 10.1080/21691401.2017.1388249.

72. Singh, R., Pochampally, R., Watabe, K., Lu, Z., and Mo, Y.Y. (2014). Exosome-mediated transfer of miR-10b promotes cell invasion in breast cancer. Mol Cancer *13*, 256. 10.1186/1476-4598-13-256.

73. Kosaka, N., Iguchi, H., Hagiwara, K., Yoshioka, Y., Takeshita, F., and Ochiya, T. (2013). Neutral sphingomyelinase 2 (nSMase2)-dependent exosomal transfer of angiogenic microRNAs regulate cancer cell metastasis. J Biol Chem *288*, 10849-10859. 10.1074/jbc.M112.446831.

74. Wei, J.X., Lv, L.H., Wan, Y.L., Cao, Y., Li, G.L., Lin, H.M., Zhou, R., Shang, C.Z., Cao, J., He, H., et al. (2015). Vps4A functions as a tumor suppressor by regulating the secretion and uptake of exosomal microRNAs in human hepatoma cells. Hepatology *61*, 1284-1294. 10.1002/hep.27660.

75. Jackson, C.E., Scruggs, B.S., Schaffer, J.E., and Hanson, P.I. (2017). Effects of Inhibiting VPS4 Support a General Role for ESCRTs in Extracellular Vesicle Biogenesis. Biophys J *113*, 1342-1352. 10.1016/j.bpj.2017.05.032.

76. Cha, D.J., Franklin, J.L., Dou, Y., Liu, Q., Higginbotham, J.N., Demory Beckler, M., Weaver, A.M., Vickers, K., Prasad, N., Levy, S., et al. (2015). KRAS-dependent sorting of miRNA to exosomes. Elife *4*, e07197. 10.7554/eLife.07197.
77. Iavello, A., Frech, V.S., Gai, C., Deregibus, M.C., Quesenberry, P.J., and Camussi, G. (2016). Role of Alix in miRNA packaging during extracellular vesicle biogenesis. Int J Mol Med *37*, 958-966. 10.3892/ijmm.2016.2488.
78. Bakirtzi, K., Man Law, I.K., Fang, K., Iliopoulos, D., and Pothoulakis, C. (2019). MiR-21 in Substance P-induced exosomes promotes cell proliferation and migration in human colonic epithelial cells. Am J Physiol Gastrointest Liver Physiol *317*, G802-G810. 10.1152/ajpgi.00043.2019.
79. Koppers-Lalic, D., Hackenberg, M., Bijnsdorp, I.V., van Eijndhoven, M.A.J., Sadek, P., Sie, D., Zini, N., Middeldorp, J.M., Ylstra, B., de Menezes, R.X., et al. (2014). Nontemplated nucleotide additions distinguish the small RNA composition in cells from exosomes. Cell Rep *8*, 1649-1658. 10.1016/j.celrep.2014.08.027.
80. Wani, S., and Kaul, D. (2018). Cancer cells govern miR-2909 exosomal recruitment through its 3'-end post-transcriptional modification. Cell Biochem Funct *36*, 106-111. 10.1002/cbf.3323.
81. Groot, M., and Lee, H. (2020). Sorting Mechanisms for MicroRNAs into Extracellular Vesicles and Their Associated Diseases. Cells *9*. 10.3390/cells9041044.
82. McKenzie, A.J., Hoshino, D., Hong, N.H., Cha, D.J., Franklin, J.L., Coffey, R.J., Patton, J.G., and Weaver, A.M. (2016). KRAS-MEK Signaling Controls Ago2 Sorting into Exosomes. Cell Rep *15*, 978-987. 10.1016/j.celrep.2016.03.085.
83. Lin, F., Zeng, Z., Song, Y., Li, L., Wu, Z., Zhang, X., Li, Z., Ke, X., and Hu, X. (2019). YBX-1 mediated sorting of miR-133 into hypoxia/reoxygenation-induced EPC-derived exosomes to

increase fibroblast angiogenesis and MEndoT. Stem Cell Res Ther *10*, 263. 10.1186/s13287-019-1377-8.

84. Shurtleff, M.J., Temoche-Diaz, M.M., Karfilis, K.V., Ri, S., and Schekman, R. (2016). Y-box protein 1 is required to sort microRNAs into exosomes in cells and in a cell-free reaction. Elife *5*. 10.7554/eLife.19276.

85. Buchet-Poyau, K., Courchet, J., Le Hir, H., Séraphin, B., Scoazec, J.Y., Duret, L., Domon-Dell, C., Freund, J.N., and Billaud, M. (2007). Identification and characterization of human Mex-3 proteins, a novel family of evolutionarily conserved RNA-binding proteins differentially localized to processing bodies. Nucleic Acids Res *35*, 1289-1300. 10.1093/nar/gkm016.

86. Lu, P., Li, H., Li, N., Singh, R.N., Bishop, C.E., Chen, X., and Lu, B. (2017). MEX3C interacts with adaptor-related protein complex 2 and involves in miR-451a exosomal sorting. PLoS One *12*, e0185992. 10.1371/journal.pone.0185992.

87. Teng, Y., Ren, Y., Hu, X., Mu, J., Samykutty, A., Zhuang, X., Deng, Z., Kumar, A., Zhang, L., Merchant, M.L., et al. (2017). MVP-mediated exosomal sorting of miR-193a promotes colon cancer progression. Nat Commun *8*, 14448. 10.1038/ncomms14448.

88. Temoche-Diaz, M.M., Shurtleff, M.J., Nottingham, R.M., Yao, J., Fadadu, R.P., Lambowitz, A.M., and Schekman, R. (2019). Distinct mechanisms of microRNA sorting into cancer cell-derived extracellular vesicle subtypes. Elife *8*. 10.7554/eLife.47544.

89. Qin, X., Guo, H., Wang, X., Zhu, X., Yan, M., Xu, Q., Shi, J., Lu, E., Chen, W., and Zhang, J. (2019). Exosomal miR-196a derived from cancer-associated fibroblasts confers cisplatin resistance in head and neck cancer through targeting CDKN1B and ING5. Genome Biol *20*, 12. 10.1186/s13059-018-1604-0.

90. Zhang, H., Deng, T., Liu, R., Ning, T., Yang, H., Liu, D., Zhang, Q., Lin, D., Ge, S., Bai, M., et al. (2020). CAF secreted miR-522 suppresses ferroptosis and promotes acquired chemo-resistance in gastric cancer. Mol Cancer *19*, 43. 10.1186/s12943-020-01168-8.
91. Gao, X., Wan, Z., Wei, M., Dong, Y., Zhao, Y., Chen, X., Li, Z., Qin, W., Yang, G., and Liu, L. (2019). Chronic myelogenous leukemia cells remodel the bone marrow niche via exosome-mediated transfer of miR-320. Theranostics *9*, 5642-5656. 10.7150/thno.34813.
92. Xu, Y.F., Xu, X., Gin, A., Nshimiyimana, J.D., Mooers, B.H.M., Caputi, M., Hannafon, B.N., and Ding, W.Q. (2020). SRSF1 regulates exosome microRNA enrichment in human cancer cells. Cell Commun Signal *18*, 130. 10.1186/s12964-020-00615-9.
93. Villarroya-Beltri, C., Gutierrez-Vazquez, C., Sanchez-Cabo, F., Perez-Hernandez, D., Vazquez, J., Martin-Cofreces, N., Martinez-Herrera, D.J., Pascual-Montano, A., Mittelbrunn, M., and Sanchez-Madrid, F. (2013). Sumoylated hnRNPA2B1 controls the sorting of miRNAs into exosomes through binding to specific motifs. Nat Commun *4*, 2980. 10.1038/ncomms3980.
94. Lee, H., Li, C., Zhang, Y., Zhang, D., Otterbein, L.E., and Jin, Y. (2019). Caveolin-1 selectively regulates microRNA sorting into microvesicles after noxious stimuli. J Exp Med *216*, 2202-2220. 10.1084/jem.20182313.
95. Wu, B., Su, S., Patil, D.P., Liu, H., Gan, J., Jaffrey, S.R., and Ma, J. (2018). Molecular basis for the specific and multivariant recognitions of RNA substrates by human hnRNP A2/B1. Nat Commun *9*, 420. 10.1038/s41467-017-02770-z.
96. Santangelo, L., Giurato, G., Cicchini, C., Montaldo, C., Mancone, C., Tarallo, R., Battistelli, C., Alonzi, T., Weisz, A., and Tripodi, M. (2016). The RNA-Binding Protein SYNCRIP Is a Component of the Hepatocyte Exosomal Machinery

Controlling MicroRNA Sorting. Cell Rep *17*, 799-808. 10.1016/j.celrep.2016.09.031.

97. Hobor, F., Dallmann, A., Ball, N.J., Cicchini, C., Battistelli, C., Ogrodowicz, R.W., Christodoulou, E., Martin, S.R., Castello, A., Tripodi, M., et al. (2018). A cryptic RNA-binding domain mediates Syncrip recognition and exosomal partitioning of miRNA targets. Nat Commun *9*, 831. 10.1038/s41467-018-03182-3.

98. Garcia-Martin, R., Wang, G., Brandao, B.B., Zanotto, T.M., Shah, S., Kumar Patel, S., Schilling, B., and Kahn, C.R. (2022). MicroRNA sequence codes for small extracellular vesicle release and cellular retention. Nature *601*, 446-451. 10.1038/s41586-021-04234-3.

99. Garbo, S., D'Andrea, D., Colantoni, A., Fiorentino, F., Mai, A., Ramos, A., Tartaglia, G.G., Tancredi, A., Tripodi, M., and Battistelli, C. (2024). m6A modification inhibits miRNAs' intracellular function, favoring their extracellular export for intercellular communication. Cell Rep *43*, 114369. 10.1016/j.celrep.2024.114369.

100. Geuens, T., Bouhy, D., and Timmerman, V. (2016). The hnRNP family: insights into their role in health and disease. Hum Genet *135*, 851-867. 10.1007/s00439-016-1683-5.

101. Chen, Q., Jin, M., Zhu, J., Xiao, Q., and Zhang, L. (2013). Functions of heterogeneous nuclear ribonucleoproteins in stem cell potency and differentiation. Biomed Res Int *2013*, 623978. 10.1155/2013/623978.

102. Dreyfuss, G., Swanson, M.S., and Pinol-Roma, S. (1988). Heterogeneous nuclear ribonucleoprotein particles and the pathway of mRNA formation. Trends Biochem Sci *13*, 86-91. 10.1016/0968-0004(88)90046-1.

103. Valverde, R., Edwards, L., and Regan, L. (2008). Structure and function of KH domains. FEBS J *275*, 2712-2726. 10.1111/j.1742-4658.2008.06411.x.

104. Makeyev, A.V., and Liebhaber, S.A. (2002). The poly(C)-binding proteins: a multiplicity of functions and a search for mechanisms. RNA *8*, 265-278. 10.1017/s1355838202024627.
105. Kiledjian, M., and Dreyfuss, G. (1992). Primary structure and binding activity of the hnRNP U protein: binding RNA through RGG box. EMBO J *11*, 2655-2664. 10.1002/j.1460-2075.1992.tb05331.x.
106. Chaudhury, A., Chander, P., and Howe, P.H. (2010). Heterogeneous nuclear ribonucleoproteins (hnRNPs) in cellular processes: Focus on hnRNP E1's multifunctional regulatory roles. RNA *16*, 1449-1462. 10.1261/rna.2254110.
107. Choi, H.S., Hwang, C.K., Song, K.Y., Law, P.Y., Wei, L.N., and Loh, H.H. (2009). Poly(C)-binding proteins as transcriptional regulators of gene expression. Biochem Biophys Res Commun *380*, 431-436. 10.1016/j.bbrc.2009.01.136.
108. Weighardt, F., Biamonti, G., and Riva, S. (1996). The roles of heterogeneous nuclear ribonucleoproteins (hnRNP) in RNA metabolism. Bioessays *18*, 747-756. 10.1002/bies.950180910.
109. Blanc, V., Navaratnam, N., Henderson, J.O., Anant, S., Kennedy, S., Jarmuz, A., Scott, J., and Davidson, N.O. (2001). Identification of GRY-RBP as an apolipoprotein B RNA-binding protein that interacts with both apobec-1 and apobec-1 complementation factor to modulate C to U editing. J Biol Chem *276*, 10272-10283. 10.1074/jbc.M006435200.
110. Mizutani, A., Fukuda, M., Ibata, K., Shiraishi, Y., and Mikoshiba, K. (2000). SYNCRIP, a cytoplasmic counterpart of heterogeneous nuclear ribonucleoprotein R, interacts with ubiquitous synaptotagmin isoforms. J Biol Chem *275*, 9823-9831. 10.1074/jbc.275.13.9823.
111. Williams, K.R., McAninch, D.S., Stefanovic, S., Xing, L., Allen, M., Li, W., Feng, Y., Mihailescu, M.R., and Bassell, G.J. (2016). hnRNP-Q1 represses nascent axon growth in cortical neurons by inhibiting Gap-43 mRNA translation. Mol Biol Cell *27*, 518-534. 10.1091/mbc.E15-07-0504.

112. Bannai, H., Fukatsu, K., Mizutani, A., Natsume, T., Iemura, S., Ikegami, T., Inoue, T., and Mikoshiba, K. (2004). An RNA-interacting protein, SYNCRIP (heterogeneous nuclear ribonuclear protein Q1/NSAP1) is a component of mRNA granule transported with inositol 1,4,5-trisphosphate receptor type 1 mRNA in neuronal dendrites. J Biol Chem *279*, 53427-53434. 10.1074/jbc.M409732200.
113. Chen, H.H., Chang, J.G., Lu, R.M., Peng, T.Y., and Tarn, W.Y. (2008). The RNA binding protein hnRNP Q modulates the utilization of exon 7 in the survival motor neuron 2 (SMN2) gene. Mol Cell Biol *28*, 6929-6938. 10.1128/MCB.01332-08.
114. Mourelatos, Z., Abel, L., Yong, J., Kataoka, N., and Dreyfuss, G. (2001). SMN interacts with a novel family of hnRNP and spliceosomal proteins. EMBO J *20*, 5443-5452. 10.1093/emboj/20.19.5443.
115. Herrejon Chavez, F., Luo, H., Cifani, P., Pine, A., Chu, E.L., Joshi, S., Barin, E., Schurer, A., Chan, M., Chang, K., et al. (2023). RNA binding protein SYNCRIP maintains proteostasis and self-renewal of hematopoietic stem and progenitor cells. Nat Commun *14*, 2290. 10.1038/s41467-023-38001-x.
116. McDermott, S.M., Yang, L., Halstead, J.M., Hamilton, R.S., Meignin, C., and Davis, I. (2014). Drosophila Syncrip modulates the expression of mRNAs encoding key synaptic proteins required for morphology at the neuromuscular junction. RNA *20*, 1593-1606. 10.1261/rna.045849.114.
117. Vu, L.P., Prieto, C., Amin, E.M., Chhangawala, S., Krivtsov, A., Calvo-Vidal, M.N., Chou, T., Chow, A., Minuesa, G., Park, S.M., et al. (2017). Functional screen of MSI2 interactors identifies an essential role for SYNCRIP in myeloid leukemia stem cells. Nat Genet *49*, 866-875. 10.1038/ng.3854.
118. Yoo, B.C., Hong, S.H., Ku, J.L., Kim, Y.H., Shin, Y.K., Jang, S.G., Kim, I.J., Jeong, S.Y., and Park, J.G. (2009). Galectin-3 stabilizes heterogeneous nuclear ribonucleoprotein Q to

maintain proliferation of human colon cancer cells. Cell Mol Life Sci *66*, 350-364. 10.1007/s00018-009-8562-3.

119. Santangelo, L., Marchetti, A., Cicchini, C., Conigliaro, A., Conti, B., Mancone, C., Bonzo, J.A., Gonzalez, F.J., Alonzi, T., Amicone, L., and Tripodi, M. (2011). The stable repression of mesenchymal program is required for hepatocyte identity: a novel role for hepatocyte nuclear factor 4α. Hepatology *53*, 2063-2074. 10.1002/hep.24280.

120. Garibaldi, F., Cicchini, C., Conigliaro, A., Santangelo, L., Cozzolino, A.M., Grassi, G., Marchetti, A., Tripodi, M., and Amicone, L. (2012). An epistatic mini-circuitry between the transcription factors Snail and HNF4α controls liver stem cell and hepatocyte features exhorting opposite regulation on stemness-inhibiting microRNAs. Cell Death Differ *19*, 937-946. 10.1038/cdd.2011.175.

121. Cicchini, C., de Nonno, V., Battistelli, C., Cozzolino, A.M., De Santis Puzzonia, M., Ciafrè, S.A., Brocker, C., Gonzalez, F.J., Amicone, L., and Tripodi, M. (2015). Epigenetic control of EMT/MET dynamics: HNF4α impacts DNMT3s through miRs-29. Biochim Biophys Acta *1849*, 919-929. 10.1016/j.bbagrm.2015.05.005.

122. Battistelli, C., Cicchini, C., Santangelo, L., Tramontano, A., Grassi, L., Gonzalez, F.J., de Nonno, V., Grassi, G., Amicone, L., and Tripodi, M. (2017). The Snail repressor recruits EZH2 to specific genomic sites through the enrollment of the lncRNA HOTAIR in epithelial-to-mesenchymal transition. Oncogene *36*, 942-955. 10.1038/onc.2016.260.

123. Battistelli, C., Sabarese, G., Santangelo, L., Montaldo, C., Gonzalez, F.J., Tripodi, M., and Cicchini, C. (2019). The lncRNA HOTAIR transcription is controlled by HNF4α-induced chromatin topology modulation. Cell Death Differ *26*, 890-901. 10.1038/s41418-018-0170-z.

124. Battistelli, C., Garbo, S., Riccioni, V., Montaldo, C., Santangelo, L., Vandelli, A., Strippoli, R., Tartaglia, G.G.,

Tripodi, M., and Cicchini, C. (2021). Design and Functional Validation of a Mutant Variant of the LncRNA. Cancer Res *81*, 103-113. 10.1158/0008-5472.CAN-20-1764.

125. Riccioni, V., Trionfetti, F., Montaldo, C., Garbo, S., Marocco, F., Battistelli, C., Marchetti, A., Strippoli, R., Amicone, L., Cicchini, C., and Tripodi, M. (2022). SYNCRIP Modulates the Epithelial-Mesenchymal Transition in Hepatocytes and HCC Cells. Int J Mol Sci *23*. 10.3390/ijms23020913.
126. Sidiqi, M., Wilce, J.A., Vivian, J.P., Porter, C.J., Barker, A., Leedman, P.J., and Wilce, M.C. (2005). Structure and RNA binding of the third KH domain of poly(C)-binding protein 1. Nucleic Acids Res *33*, 1213-1221. 10.1093/nar/gki265.
127. Du, Z., Lee, J.K., Tjhen, R., Li, S., Pan, H., Stroud, R.M., and James, T.L. (2005). Crystal structure of the first KH domain of human poly(C)-binding protein-2 in complex with a C-rich strand of human telomeric DNA at 1.7 A. J Biol Chem *280*, 38823-38830. 10.1074/jbc.M508183200.
128. Chkheidze, A.N., and Liebhaber, S.A. (2003). A novel set of nuclear localization signals determine distributions of the alphaCP RNA-binding proteins. Mol Cell Biol *23*, 8405-8415. 10.1128/MCB.23.23.8405-8415.2003.
129. Thakur, S., Nakamura, T., Calin, G., Russo, A., Tamburrino, J.F., Shimizu, M., Baldassarre, G., Battista, S., Fusco, A., Wassell, R.P., et al. (2003). Regulation of BRCA1 transcription by specific single-stranded DNA binding factors. Mol Cell Biol *23*, 3774-3787. 10.1128/MCB.23.11.3774-3787.2003.
130. Yuan, C., Chen, M., and Cai, X. (2021). Advances in poly(rC)-binding protein 2: Structure, molecular function, and roles in cancer. Biomed Pharmacother *139*, 111719. 10.1016/j.biopha.2021.111719.
131. Zhang, Y., Si, Y., Ma, N., and Mei, J. (2015). The RNA-binding protein PCBP2 inhibits Ang II-induced hypertrophy of cardiomyocytes though promoting GPR56 mRNA

degeneration. Biochem Biophys Res Commun *464*, 679-684. 10.1016/j.bbrc.2015.06.139.

132. Evans, J.R., Mitchell, S.A., Spriggs, K.A., Ostrowski, J., Bomsztyk, K., Ostarek, D., and Willis, A.E. (2003). Members of the poly (rC) binding protein family stimulate the activity of the c-myc internal ribosome entry segment in vitro and in vivo. Oncogene *22*, 8012-8020. 10.1038/sj.onc.1206645.

133. Ogram, S.A., Spear, A., Sharma, N., and Flanegan, J.B. (2010). The 5'CL-PCBP RNP complex, 3' poly(A) tail and 2A(pro) are required for optimal translation of poliovirus RNA. Virology *397*, 14-22. 10.1016/j.virol.2009.11.006.

134. Leidgens, S., Bullough, K.Z., Shi, H., Li, F., Shakoury-Elizeh, M., Yabe, T., Subramanian, P., Hsu, E., Natarajan, N., Nandal, A., et al. (2013). Each member of the poly-r(C)-binding protein 1 (PCBP) family exhibits iron chaperone activity toward ferritin. J Biol Chem *288*, 17791-17802. 10.1074/jbc.M113.460253.

135. Frey, A.G., Nandal, A., Park, J.H., Smith, P.M., Yabe, T., Ryu, M.S., Ghosh, M.C., Lee, J., Rouault, T.A., Park, M.H., and Philpott, C.C. (2014). Iron chaperones PCBP1 and PCBP2 mediate the metallation of the dinuclear iron enzyme deoxyhypusine hydroxylase. Proc Natl Acad Sci U S A *111*, 8031-8036. 10.1073/pnas.1402732111.

136. Zhang, X., Hua, L., Yan, D., Zhao, F., Liu, J., Zhou, H., Wu, M., Zhang, C., Chen, Y., Chen, B., and Hu, B. (2016). Overexpression of PCBP2 contributes to poor prognosis and enhanced cell growth in human hepatocellular carcinoma. Oncol Rep *36*, 3456-3464. 10.3892/or.2016.5167.

137. Liu, Y., Zhang, X., Lin, J., Chen, Y., Qiao, Y., Guo, S., Yang, Y., Zhu, G., Pan, Q., Wang, J., and Sun, F. (2019). CCT3 acts upstream of YAP and TFCP2 as a potential target and tumour biomarker in liver cancer. Cell Death Dis *10*, 644. 10.1038/s41419-019-1894-5.

138. Luo, K., and Zhuang, K. (2017). High expression of PCBP2 is associated with progression and poor prognosis in patients with glioblastoma. Biomed Pharmacother *94*, 659-665. 10.1016/j.biopha.2017.07.103.
139. Tang, S.L., Gao, Y.L., and Chen, X.B. (2015). MicroRNA-214 targets PCBP2 to suppress the proliferation and growth of glioma cells. Int J Clin Exp Pathol *8*, 12571-12576.
140. Lin, X., Yang, B., Liu, W., Tan, X., Wu, F., Hu, P., Jiang, T., Bao, Z., Yuan, J., Qiang, B., et al. (2016). Interplay between PCBP2 and miRNA modulates ARHGDIA expression and function in glioma migration and invasion. Oncotarget *7*, 19483-19498. 10.18632/oncotarget.6869.
141. Hu, C.E., Liu, Y.C., Zhang, H.D., and Huang, G.J. (2014). The RNA-binding protein PCBP2 facilitates gastric carcinoma growth by targeting miR-34a. Biochem Biophys Res Commun *448*, 437-442. 10.1016/j.bbrc.2014.04.124.
142. Guantario, B., Conigliaro, A., Amicone, L., Sambuy, Y., and Bellovino, D. (2012). The new murine hepatic 3A cell line responds to stress stimuli by activating an efficient Unfolded Protein Response (UPR). Toxicol In Vitro *26*, 7-15. 10.1016/j.tiv.2011.09.020.
143. Mancone, C., Montaldo, C., Santangelo, L., Di Giacomo, C., Costa, V., Amicone, L., Ippolito, G., Pucillo, L.P., Alonzi, T., and Tripodi, M. (2012). Ferritin heavy chain is the host factor responsible for HCV-induced inhibition of apoB-100 production and is required for efficient viral infection. J Proteome Res *11*, 2786-2797. 10.1021/pr201128s.
144. Pasque, V., Gillich, A., Garrett, N., and Gurdon, J.B. (2011). Histone variant macroH2A confers resistance to nuclear reprogramming. EMBO J *30*, 2373-2387. 10.1038/emboj.2011.144.
145. Kozomara, A., Birgaoanu, M., and Griffiths-Jones, S. (2019). miRBase: from microRNA sequences to function. Nucleic Acids Res *47*, D155-D162. 10.1093/nar/gky1141.

146. Grant, C.E., Bailey, T.L., and Noble, W.S. (2011). FIMO: scanning for occurrences of a given motif. Bioinformatics *27*, 1017-1018. 10.1093/bioinformatics/btr064.
147. Shi, J., Dong, M., Li, L., Liu, L., Luz-Madrigal, A., Tsonis, P.A., Del Rio-Tsonis, K., and Liang, C. (2015). mirPRo-a novel standalone program for differential expression and variation analysis of miRNAs. Sci Rep *5*, 14617. 10.1038/srep14617.
148. Li, H., and Homer, N. (2010). A survey of sequence alignment algorithms for next-generation sequencing. Brief Bioinform *11*, 473-483. 10.1093/bib/bbq015.
149. Love, M.I., Huber, W., and Anders, S. (2014). Moderated estimation of fold change and dispersion for RNA-seq data with DESeq2. Genome Biol *15*, 550. 10.1186/s13059-014-0550-8.
150. Cook, K.B., Kazan, H., Zuberi, K., Morris, Q., and Hughes, T.R. (2011). RBPDB: a database of RNA-binding specificities. Nucleic Acids Res *39*, D301-308. 10.1093/nar/gkq1069.
151. Liao, J.Y., Yang, B., Zhang, Y.C., Wang, X.J., Ye, Y., Peng, J.W., Yang, Z.Z., He, J.H., Zhang, Y., Hu, K., et al. (2020). EuRBPDB: a comprehensive resource for annotation, functional and oncological investigation of eukaryotic RNA binding proteins (RBPs). Nucleic Acids Res *48*, D307-D313. 10.1093/nar/gkz823.
152. Ray, D., Kazan, H., Cook, K.B., Weirauch, M.T., Najafabadi, H.S., Li, X., Gueroussov, S., Albu, M., Zheng, H., Yang, A., et al. (2013). A compendium of RNA-binding motifs for decoding gene regulation. Nature *499*, 172-177. 10.1038/nature12311.
153. Treiber, T., Treiber, N., Plessmann, U., Harlander, S., Daiss, J.L., Eichner, N., Lehmann, G., Schall, K., Urlaub, H., and Meister, G. (2017). A Compendium of RNA-Binding Proteins that Regulate MicroRNA Biogenesis. Mol Cell *66*, 270-284 e213. 10.1016/j.molcel.2017.03.014.
154. Van Nostrand, E.L., Freese, P., Pratt, G.A., Wang, X., Wei, X., Xiao, R., Blue, S.M., Chen, J.Y., Cody, N.A.L., Dominguez, D.,

et al. (2020). A large-scale binding and functional map of human RNA-binding proteins. Nature *583*, 711-719. 10.1038/s41586-020-2077-3.

155. Fonseca, B.D., Zakaria, C., Jia, J.J., Graber, T.E., Svitkin, Y., Tahmasebi, S., Healy, D., Hoang, H.D., Jensen, J.M., Diao, I.T., et al. (2015). La-related Protein 1 (LARP1) Represses Terminal Oligopyrimidine (TOP) mRNA Translation Downstream of mTOR Complex 1 (mTORC1). J Biol Chem *290*, 15996-16020. 10.1074/jbc.M114.621730.
156. Wickham, L., Duchaine, T., Luo, M., Nabi, I.R., and DesGroseillers, L. (1999). Mammalian staufen is a double-stranded-RNA- and tubulin-binding protein which localizes to the rough endoplasmic reticulum. Mol Cell Biol *19*, 2220-2230. 10.1128/MCB.19.3.2220.
157. Ishii, T., Igawa, T., Hayakawa, H., Fujita, T., Sekiguchi, M., and Nakabeppu, Y. (2020). PCBP1 and PCBP2 both bind heavily oxidized RNA but cause opposing outcomes, suppressing or increasing apoptosis under oxidative conditions. J Biol Chem *295*, 12247-12261. 10.1074/jbc.RA119.011870.
158. Makeyev, A.V., Chkheidze, A.N., and Liebhaber, S.A. (1999). A set of highly conserved RNA-binding proteins, alphaCP-1 and alphaCP-2, implicated in mRNA stabilization, are coexpressed from an intronless gene and its intron-containing paralog. J Biol Chem *274*, 24849-24857. 10.1074/jbc.274.35.24849.
159. Perrotti, D., Cesi, V., Trotta, R., Guerzoni, C., Santilli, G., Campbell, K., Iervolino, A., Condorelli, F., Gambacorti-Passerini, C., Caligiuri, M.A., and Calabretta, B. (2002). BCR-ABL suppresses C/EBPalpha expression through inhibitory action of hnRNP E2. Nat Genet *30*, 48-58. 10.1038/ng791.
160. Yabe-Wada, T., Philpott, C.C., and Onai, N. (2020). PCBP2 post-transcriptionally regulates sortilin expression by

binding to a C-rich element in its 3' UTR. FEBS Open Bio *10*, 407-413. 10.1002/2211-5463.12794.

161. Yuan, L., Xiao, Y., Zhou, Q., Yuan, D., Wu, B., Chen, G., and Zhou, J. (2014). Proteomic analysis reveals that MAEL, a component of nuage, interacts with stress granule proteins in cancer cells. Oncol Rep *31*, 342-350. 10.3892/or.2013.2836.
162. Zhang, P., Cao, M., Zhang, Y., Xu, L., Meng, F., Wu, X., Xia, T., Chen, Q., Shi, G., Wu, P., et al. (2020). A novel antisense lncRNA NT5E promotes progression by modulating the expression of SYNCRIP and predicts a poor prognosis in pancreatic cancer. J Cell Mol Med *24*, 10898-10912. 10.1111/jcmm.15718.
163. Broermann, A., Schmid, R., Gabrielyan, O., Sakowski, M., Eisele, C., Keller, S., Wolff, M., Baum, P., Stierstorfer, B., Huber, J., et al. (2020). Exosomal miRNAs as Potential Biomarkers to Monitor Phosphodiesterase 5 Inhibitor Induced Anti-Fibrotic Effects on CCl(4) Treated Rats. Int J Mol Sci *22*. 10.3390/ijms22010382.
164. Dosil, S.G., Lopez-Cobo, S., Rodriguez-Galan, A., Fernandez-Delgado, I., Ramirez-Huesca, M., Milan-Rois, P., Castellanos, M., Somoza, A., Gomez, M.J., Reyburn, H.T., et al. (2022). Natural killer (NK) cell-derived extracellular-vesicle shuttled microRNAs control T cell responses. Elife *11*. 10.7554/eLife.76319.
165. Jiao, Y., Xu, P., Shi, H., Chen, D., and Shi, H. (2021). Advances on liver cell-derived exosomes in liver diseases. J Cell Mol Med *25*, 15-26. 10.1111/jcmm.16123.
166. Zhao, Y., Liu, J., Xiong, Z., Gu, S., and Xia, X. (2024). Exosome-derived miR-23a-5p inhibits HCC proliferation and angiogenesis by regulating PRDX2 expression: MiR-23a-5p/PRDX2 axis in HCC progression. Heliyon *10*, e23168. 10.1016/j.heliyon.2023.e23168.

PAPERS ACCEPTED OR SUBMITTED DURING PhD COURSE

1) Riccioni, V., Trionfetti, F., Montaldo, C., Garbo, S., Marocco, F., Battistelli, C., Marchetti, A., Strippoli, R., Amicone, L., Cicchini, C., and Tripodi, M. (2022). SYNCRIP Modulates the Epithelial-Mesenchymal Transition in Hepatocytes and HCC Cells. Int J Mol Sci *23*. 10.3390/ijms23020913

2) Pyka P, Haberek W, Więcek M, Szymanska E, Ali W, Cios A, Jastrzębska-Więsek M, Satała G, Podlewska S, Di Giacomo S, Di Sotto A, Garbo S, Karcz T, Lambona C, Marocco F, Latacz G, Sudoł-Tałaj S, Mordyl B, Głuch-Lutwin M, Siwek A, Czarnota-Łydka K, Gogola D, Olejarz-Maciej A, Wilczyńska-Zawal N, Honkisz-Orzechowska E, Starek M, Dąbrowska M, Kucwaj-Brysz K, Fioravanti R, Nasim MJ, Hittinger M, Partyka A, Wesołowska A, Battistelli C, Zwergel C, Handzlik J. First-in-Class Selenium-Containing Potent Serotonin Receptor 5-HT_6 Agents with a Beneficial Neuroprotective Profile against Alzheimer's Disease. J Med Chem. 2024 Jan 25;67(2):1580-1610. doi: 10.1021/acs.jmedchem.3c02148.

3) Marocco F., Garbo S., Montaldo C., Colantoni A., Luca Quattrocchi L., Gaboardi G., Cicchini C., Gian Gaetano Tartaglia G.G., Battistelli C. and Tripodi M. Negative regulation of miRNAs sorting in EVs: the RNA-binding protein PCBP2 impairs SYNCRIP-mediated miRNAs EVs loading. *(under review)*